Available online at www.sciencedirect.com

ScienceDirect

Journal of Differential Equations 346 (2023) 64–107

Journal of Differential Equations

www.elsevier.com/locate/jde

Hopf bifurcation for general network-organized reaction-diffusion systems and its application in a multi-patch predator-prey system

Wei Gou [a], Zhen Jin [b,c,*], Hao Wang [d]

[a] *School of Science, North University of China, Taiyuan, Shanxi 030051, China*

[b] *Complex Systems Research Center, Shanxi University, Taiyuan, Shanxi 030006, China*

[c] *Shanxi Key Laboratory of Mathematical Technique and Big Data Analysis on Disease Control and Prevention, Shanxi University, Taiyuan, Shanxi 030006, China*

[d] *Department of Mathematical and Statistical Sciences, University of Alberta, Edmonton, AB T6G 2G1, Canada*

Received 1 November 2020; revised 18 April 2022; accepted 15 November 2022

Abstract

For decades, the network-organized reaction-diffusion models have been widely used to study ecological and epidemiological phenomena in discrete space. However, the high dimensionality of these nonlinear systems places a long-standing restriction to develop the normal forms of various bifurcations. In this paper, we take an important step to present a rigorous procedure for calculating the normal form associated with the Hopf bifurcation of the general network-organized reaction-diffusion systems, which is similar to but can be much more intricate than the corresponding procedure for the extensively explored PDE systems. To show the potential applications of our obtained theoretical results, we conduct the detailed Hopf bifurcation analysis for a multi-patch predator-prey system defined on any undirected connected underlying network and on the particular non-periodic one-dimensional lattice network. Remarkably, we reveal that the structure of the underlying network imposes a significant effect on the occurrence of the spatially nonhomogeneous Hopf bifurcations.

MSC: 34C23; 37G10; 92D40

* Corresponding author at: Complex Systems Research Center, Shanxi University, Taiyuan, Shanxi 030006, China.
E-mail address: jinzhn@263.net (Z. Jin).

https://doi.org/10.1016/j.jde.2022.11.026
0022-0396/

Keywords: Complex network; Reaction-diffusion process; Hopf bifurcation; Spatially nonhomogeneous periodic solutions; Multi-patch predator-prey system

1. Introduction

Many realistic reaction-diffusion processes take place in discrete space, rather than in continuous space, such as the population dynamics and evolution in fragmented landscapes [18,14], and the spread of infectious diseases among cities or urban areas [32,38]. Under the basic assumption that interacting species or sub-populations occupy network nodes representing the isolated discrete locations, and diffuse across the dispersal links, the network-organized reaction-diffusion modeling approach has become an increasingly essential framework to understand the intrinsic mechanisms and to develop effective strategies for ecological management and protection as well as disease prevention and control [23,10]. The spatially structured metapopulation models in ecology with dispersal connection between habitats allow exploring population dynamics including stability and persistence under spatial connectivity and individual movement [19,9]. The metapopulation epidemic model in transportation networks is another excellent example for the network-organized reaction-diffusion models, whose threshold dynamics have been extensively studied in literatures [1,7,36]. In the 21st century, the network-based metapopulation approach has also been revamped in data-driven large-scale simulations and forecasting for the spread of infectious diseases [8,5].

In the network-organized reaction-diffusion models from ecology, epidemiology and other fields, network architecture usually results in the high dimensionality of these large systems, and thereby leads to grievous restrictions on the dynamical analysis of such spatial network models, which severely limits the broad applications of this fundamental class of discrete-space models. On the contrary, once these restrictions are broken through, great progress will be hopeful to accomplish. This conclusion can be easily obtained once we review the research of Turing patterns in networks. As early as 1971, Othmer and Scriven [26] pointed out that Turing instability could emerge in the network-organized reaction-diffusion models with proposing a general mathematical framework for the analysis of this instability. In the following several decades, this research was limited to regular lattices or small networks [27,31]. In 2010, Nakao and Mikhailov [25] conducted a landmark research of Turing patterns in large random complex networks, and their work has already triggered many follow-up investigations in this direction. In the past decade, abundant stationary Turing patterns found in various networks have largely expanded the understanding of spatial self-organizations [30,11,17,12]. Besides stationary Turing patterns, Turing-like traveling waves (oscillatory Turing patterns) also gain some attention. Hata et al. [16] studied oscillatory Turing instabilities for all possible food webs with three predator or prey species and revealed that no wave patterns existed in networks but there existed spontaneous development of heterogeneous oscillations and possible extinction of species. Asllani et al. [2] demonstrated the existence of traveling waves in the balanced directed networks, which is impossible in undirected networks under same conditions. Petit and his collaborators [29,28] showed the delay-induced Turing-like waves for one-species and two-species reaction-diffusion models on networks. Later, Chang et al. [6] studied a Leslie-Gower Holling-type III predator-prey model with a single discrete-time delay defined on networks and discussed the influences of network topology on delay-induced wave patterns in the aspects of amplitude and period.

The above research works about the stationary Turing patterns and the Turing-like traveling waves are obtained by determining the corresponding Turing instability and oscillatory Turing instability via a linear stability analysis. The method is to expand the heterogeneous perturbations over the set of Laplacian eigenvectors of one certain underlying network [26,25]. However, this is not sufficient for uncovering complex dynamical behaviors of the general network-organized reaction-diffusion systems. As we all know, the normal form theory, together with the central manifold method, has been widely applied to discover the complex dynamical behaviors in ordinary differential equations (ODEs) [22] and partial differential equations (PDEs) [15,39,33,35]. Currently, the research on complex dynamical behaviors of the network-organized reaction-diffusion systems, as one kind of high dimensional ODEs, is yet far less extensive and in-depth than that of their corresponding parabolic PDEs. It is important and intriguing to establish the normal form theory of the steady-state bifurcation, the Hopf bifurcation [39] and the Turing-Hopf bifurcation [33], and other types of bifurcations for the network-organized reaction-diffusion systems to uncover the complex dynamical behaviors.

To the best of our knowledge, a promising progress has not been made until recently by Tian et al. [37,34]. Based on the orthogonality of Laplacian eigenvectors of the underlying network, they utilized a linear stability analysis and a center manifold theory to determine the direction and stability of the Hopf bifurcations in some specific network-organized reaction-diffusion models in the presence or absence of a time delay. However, they still did not establish any abstract Hopf bifurcation theorem for the general network-organized reaction-diffusion systems. Furthermore, their application of the orthogonality of Laplacian eigenvectors to transform the original systems lacks rigorous mathematical proofs, at least up to now.

In this paper, without following these previous works, we make a lot of effort to strictly derive the normal form of Hopf bifurcation for the general two-species network-organized reaction-diffusion systems according to the basic Hopf bifurcation theory. With the aid of Kronecker product, we demonstrate the fundamental Theorem 2.1, which manifests the eigenvalues and their associated eigenvectors of the high dimensional Jacobian matrix at one homogeneous equilibrium of the considered system, for the first time. This critical theorem allows strictly developing the Hopf bifurcation Theorem 2.2 for the general two-species homogeneous network-organized reaction-diffusion systems. Our theorem mainly reveals that the procedure for calculating the normal form associated with the Hopf bifurcation in interest is similar to but can be more intricate than the corresponding procedure for the PDE system provided in [15,39]. Generally, the unexpected difficulty lies in getting the analytic expressions for computing the important quantity $\mathrm{Re}(c_1(\mu_0))$ to determine their bifurcation direction of the possible bifurcating spatially nonhomogeneous periodic solutions, which needs to be handled by some numerical calculations.

To show the potential applicability of the established theorem, we provide a rigorous study of the Hopf bifurcation for a multi-patch predator-prey system, which can be defined on any underlying network. When this illustrative system is defined on the special non-periodic one-dimensional lattice network, it is equivalent to one spatially semidiscrete approximating system of the corresponding reaction-diffusion system subject to Neumann boundary conditions on one-dimensional spatial domain, with a necessary rescaling of the diffusion rates. Following the intuition, the Hopf bifurcation results in this particular case are in good agreement with the ones of the corresponding PDE model studied in [39]. Meanwhile, we derive the analytic expressions for computing quantity $\mathrm{Re}(c_1(\mu_0))$ of its bifurcating spatially nonhomogeneous periodic solutions, although they are of different forms.

However, once our illustrative system is defined on other types of connected undirected networks, the occurrence and properties of spatially nonhomogeneous periodic solutions yet exhibit substantial differences, which might suggest some significant ecological laws for population dynamics. In mathematics, it yet becomes a challenge to obtain the analytic expressions for computing quantity $\mathrm{Re}(c_1(\mu_0))$ of the possible bifurcating spatially nonhomogeneous periodic solutions. In addition, the decreasing of negative Laplacian eigenvalues of underlying networks can reduce the number of the possible spatially nonhomogeneous Hopf bifurcation points. Basically, our analytical results confirm an ecological conclusion that a sufficiently small diffusion rate will promote the spatially nonhomogeneous distribution of populations in network (discrete space) by weakening diffusion coupling among nodes. We further reveal that the nonlocal connected edges, the rewired stochastic edges, and the hub nodes with large connectivity in underlying networks will directly or indirectly suppress the spatial heterogeneity of population distribution.

The remaining parts of this paper are structured as follows. In Section 2, we develop the Hopf bifurcation theorem for the general two-species network-organized reaction-diffusion systems. In Section 3, we apply the obtained theoretical results to the Hopf bifurcation analysis of a multi-patch predator-prey system defined on any underlying connected undirected network and on the particular non-periodic one-dimensional lattice network. In Section 4, we provide four typical examples and a group of numerical simulations to illustrate the effects of network topology on the occurrence of spatially nonhomogeneous Hopf bifurcations. We finally summarize and discuss our findings in Section 5.

2. Normal form of Hopf bifurcation for general network-organized reaction-diffusion systems

We consider a general network-organized reaction-diffusion system defined on a certain underlying network G of size N:

$$\begin{cases} \frac{d}{dt}u_i(t) = f(\mu, u_i, v_i) + d_u \sum\limits_{j=1}^{N} L_{ij}u_j, \\ \frac{d}{dt}v_i(t) = g(\mu, u_i, v_i) + d_v \sum\limits_{j=1}^{N} L_{ij}v_j, \end{cases} \tag{2.1}$$

for $i = 1, \ldots, N$, where u_i and v_i are local densities on node i of species u and v. System (2.1) takes the consideration that there are two different species u and v living on discrete nodes and diffusing over links between them with their respective diffusion constants denoted as $d_u,\ d_v \in \mathbb{R}^+$. The local dynamics of species u and v are specified by the functions $f(u, v)$ and $g(u, v)$, and the diffusive fluxes of them are correspondingly expressed as $d_u \sum_{j=1}^{N} L_{ij}u_j$ and $d_v \sum_{j=1}^{N} L_{ij}v_j$, with L_{ij} being the elements of network Laplacian matrix $\boldsymbol{L}$. The Laplacian matrix $\boldsymbol{L}$ is defined as $L_{ij} = A_{ij} - k_i\delta_{ij}$, where A_{ij} are the elements of the adjacency matrix $\boldsymbol{A}$ taking $A_{ij} = 1$ if node i and j $(i, j = 1, \ldots, N)$ are connected $i \neq j$ and $A_{ij} = 0$ otherwise, $k_i = \sum_{j=1}^{N} A_{ij}$ is the degree of node i, and δ_{ij} is the Kronecker delta function, such that $\delta_{ij} = 0$ for $i \neq j$ and 1 otherwise. Notice that in (2.1), the Laplacian matrix $\boldsymbol{L}$ describes the diffusion of species following the well-known Fick's law as the Laplacian operator Δ in the reaction-diffusion systems in classical continuous media [25].

Here, $\mu \in \mathbb{R}$ is introduced as the bifurcation parameter, and without loss of generality, we assume that $f,\ g : \mathbb{R} \times \mathbb{R}^2 \to \mathbb{R}$ are $C^k (k \geq 3)$ with $f(\mu, 0, 0) = g(\mu, 0, 0) = 0$. Therefore, system (2.1) admits a homogeneous equilibrium $E_\mu : (\mu, u_i, v_i) = (\mu, 0, 0)$ for $i = 1, 2, \ldots, N$ and all μ. Around the equilibrium E_μ, the linearized system of (2.1) is

$$
\begin{cases} \frac{d}{dt}u_i(t) = A(\mu)u_i + B(\mu)v_i + d_u \sum\limits_{j=1}^{N} L_{ij}u_j, \\ \frac{d}{dt}v_i(t) = C(\mu)u_i + D(\mu)v_i + d_v \sum\limits_{j=1}^{N} L_{ij}v_j, \end{cases} \tag{2.2}
$$

where $A(\mu) = f_u(\mu, 0, 0)$, $B(\mu) = f_v(\mu, 0, 0)$, $C(\mu) = g_u(\mu, 0, 0)$, $D(\mu) = g_v(\mu, 0, 0)$.

By introducing the vector $\boldsymbol{U}(t) := \big(u_1(t), v_1(t), \cdots\cdots, u_N(t), v_N(t)\big)^T$, system (2.2) can be written as the matrix form

$$
\frac{d\boldsymbol{U}}{dt} = \big(\boldsymbol{I}_N \otimes \boldsymbol{K}(\mu)\big)\boldsymbol{U} + \big(\boldsymbol{L} \otimes \boldsymbol{D}\big)\boldsymbol{U}, \tag{2.3}
$$

where $\boldsymbol{K}(\mu) = \begin{pmatrix} A(\mu) & B(\mu) \\ C(\mu) & D(\mu) \end{pmatrix}$, $\boldsymbol{D} = \begin{pmatrix} d_u & 0 \\ 0 & d_v \end{pmatrix}$, $\boldsymbol{I}_N$ is the $N \times N$ identity matrix, and $\otimes$ denotes the Kronecker product (i.e., the direct product or tensor product) [13]. Apparently, the stability of this linear system is determined by the eigenvalues of Jacobian matrix

$$
\boldsymbol{M}(\mu) := \boldsymbol{I}_N \otimes \boldsymbol{K}(\mu) + \boldsymbol{L} \otimes \boldsymbol{D}. \tag{2.4}
$$

Actually, for the eigenvalues of matrix $\boldsymbol{M}(\mu)$, it is easy to check the following theorem.

Theorem 2.1. *For the defined mode matrices*

$$
\boldsymbol{M}_l(\mu) = \boldsymbol{K}(\mu) + \Lambda_l \boldsymbol{D} \tag{2.5}
$$

for $l = 1, 2, \cdots, N$, if $\boldsymbol{M}_l(\mu)$ has the eigenvalue λ_l with the corresponding eigenvector $C_l = \big(C_{l1}, C_{l2}\big)^T$ satisfying the condition $\boldsymbol{M}_l(\mu)C_l = \lambda_l C_l$, then λ_l is the eigenvalue of $\boldsymbol{M}(\mu)$, and the corresponding eigenvector is given as $\boldsymbol{\phi}^{(l)} \otimes C_l$. Here, Λ_l are eigenvalues of Laplacian matrix $\boldsymbol{L}$ with corresponding eigenvectors $\boldsymbol{\phi}^{(l)} = \big(\phi_1^{(l)}, \phi_2^{(l)}, \cdots, \phi_N^{(l)}\big)^T$, which are determined by $\boldsymbol{L}\boldsymbol{\phi}^{(l)} = \Lambda_l \boldsymbol{\phi}^{(l)}$, that is, $\sum_{j=1}^{N} L_{ij}\phi_j^{(l)} = \Lambda_l \phi_i^{(l)}$ for $i, l = 1, 2, \cdots, N$.

Proof. Direct computation shows that for $l = 1, 2, \cdots, N$,

$$
\begin{aligned}
\boldsymbol{M}(\mu)(\boldsymbol{\phi}^{(l)} \otimes C_l) &= (\boldsymbol{I}_N \otimes \boldsymbol{K}(\mu) + \boldsymbol{L} \otimes \boldsymbol{D})(\boldsymbol{\phi}^{(l)} \otimes C_l) \\
&= (\boldsymbol{I}_N \otimes \boldsymbol{K}(\mu))(\boldsymbol{\phi}^{(l)} \otimes C_l) + (\boldsymbol{L} \otimes \boldsymbol{D})(\boldsymbol{\phi}^{(l)} \otimes C_l) \\
&= (\boldsymbol{I}_N \boldsymbol{\phi}^{(l)}) \otimes (\boldsymbol{K}(\mu)C_l) + (\boldsymbol{L}\boldsymbol{\phi}^{(l)}) \otimes (\boldsymbol{D}C_l) \\
&= \boldsymbol{\phi}^{(l)} \otimes (\boldsymbol{K}(\mu)C_l) + (\Lambda_l \boldsymbol{\phi}^{(l)}) \otimes (\boldsymbol{D}C_l) \\
&= \boldsymbol{\phi}^{(l)} \otimes (\boldsymbol{K}(\mu)C_l) + \boldsymbol{\phi}^{(l)} \otimes \big((\Lambda_l \boldsymbol{D})C_l\big) \\
&= \boldsymbol{\phi}^{(l)} \otimes \big(\boldsymbol{K}(\mu)C_l + (\Lambda_l \boldsymbol{D})C_l\big) \\
&= \boldsymbol{\phi}^{(l)} \otimes \big((\boldsymbol{K}(\mu) + \Lambda_l \boldsymbol{D})C_l\big) \\
&= \boldsymbol{\phi}^{(l)} \otimes \big(\boldsymbol{M}_l(\mu)C_l\big)
\end{aligned}
$$

$$
\begin{aligned}
&= \boldsymbol{\phi}^{(l)} \otimes \big(\lambda_l C_l\big) \\
&= \lambda_l \boldsymbol{\phi}^{(l)} \otimes C_l.
\end{aligned}
$$

That is, $\boldsymbol{M}(\mu)(\boldsymbol{\phi}^{(l)} \otimes C_l) = \lambda_l(\boldsymbol{\phi}^{(l)} \otimes C_l)$. $\square$

We note that the Laplacian matrix $\boldsymbol{L}$ of the underlying undirected network G is a real, symmetric and negative semi-definite matrix. Therefore, all eigenvalues of $\boldsymbol{L}$ are real and non-positive, and their eigenvectors can be orthonormalized as $\sum_{l=1}^{N} \phi_l^{(i)} \phi_l^{(j)} = \delta_{i,j}$ where $i, j = 1, 2, \ldots, N$. With the additional assumption that the underlying network is connected, equivalently Laplacian matrix $\boldsymbol{L}$ is also irreducible, we can further sort the indices $\{l\}$ in the decreasing order of eigenvalues such that the condition $0 = \Lambda_1 > \Lambda_2 \geq \cdots \geq \Lambda_N$ holds. Due to the fact that the multiplicity of eigenvalue $\Lambda_1 = 0$ is equal to the number of connected components of the network [4], we here emphasize $\Lambda_1 > \Lambda_2$.

According to the basic Hopf bifurcation theorem in [22,15,39], we provide the Hopf bifurcation condition for system (2.1):

(H_1) For some $\mu_0 \in \mathbb{R}$, there exists a neighborhood O of μ_0 such that for $\mu \in O$, $\boldsymbol{M}(\mu)$ has a pair of complex, simple, conjugate eigenvalues $\alpha(\mu) \pm i\omega(\mu)$, continuously differentiable in μ, with $\alpha(\mu_0) = 0$, $\omega(\mu_0) = \omega_0 > 0$, and $\alpha'(\mu_0) \neq 0$; all other eigenvalues of $\boldsymbol{M}(\mu)$ have non-zero real parts for $\mu \in O$.

According to Theorem 2.1, the eigenvalues of $\boldsymbol{M}(\mu)$ are given by the eigenvalues of $\boldsymbol{M}_l(\mu)$ for $l = 1, 2, \cdots, N$. Actually, the characteristic equation of $\boldsymbol{M}_l(\mu)$ is

$$
\lambda^2 - \lambda T_l(\mu) + D_l(\mu) = 0, \tag{2.6}
$$

where

$$
\begin{cases}
T_l(\mu) = A(\mu) + D(\mu) + \Lambda_l(d_u + d_v), \\
D_l(\mu) = \Lambda_l^2 d_u d_v + \Lambda_l\big(d_v A(\mu) + d_u D(\mu)\big) + A(\mu)D(\mu) - B(\mu)C(\mu),
\end{cases}
$$

and the eigenvalues $\lambda(\mu)$ are given by

$$
\lambda(\mu) = \frac{T_l(\mu) \pm \sqrt{T_l^2(\mu) - 4D_l(\mu)}}{2}, \tag{2.7}
$$

for $l = 1, 2, \cdots, N$. Therefore, the Hopf bifurcation condition (H_1) implies that at $\mu = \mu_0$, $\boldsymbol{M}(\mu)$ has a pair of simple purely imaginary eigenvalues $\pm i\omega_0$ if and only if there exists a unique $n \in \{1, 2, \cdots, N\}$ such that $\pm i\omega_0$ are the purely imaginary eigenvalues of $\boldsymbol{M}_n(\mu_0)$. We denote the associated eigenvector by $\boldsymbol{q} = (a_n\phi_1^{(n)}, b_n\phi_1^{(n)}, \ldots, \ldots, a_n\phi_N^{(n)}, b_n\phi_N^{(n)})^T = \boldsymbol{\phi}^{(n)} \otimes \big(a_n, b_n\big)^T$, with $a_n, b_n \in \mathbb{C}$ satisfying $\boldsymbol{M}_n(\mu_0)\big(a_n, b_n\big)^T = i\omega_0\big(a_n, b_n\big)^T$ such that $\boldsymbol{M}(\mu_0)\boldsymbol{q} = i\omega_0\boldsymbol{q}$.

By adapting the framework in Chapter 5 of [22], we rewrite system (2.1) in the abstract form

$$
\frac{d\boldsymbol{U}}{dt} = \boldsymbol{M}(\mu)\boldsymbol{U} + \boldsymbol{F}(\mu, \boldsymbol{U}), \tag{2.8}
$$

where

$$\boldsymbol{F}(\mu, \boldsymbol{U}) = \Big(\cdots, f(\mu, u_i, v_i) - A(\mu)u_i - B(\mu)v_i, g(\mu, u_i, v_i) - C(\mu)u_i - D(\mu)v_i, \cdots \Big)^T. \tag{2.9}$$

For simplicity of notations, we introduce a new expression to represent $\boldsymbol{F}(\mu, \boldsymbol{U})$ as

$$\boldsymbol{F}(\mu, \boldsymbol{U}) := \operatorname{col} \begin{pmatrix} f(\mu, u_i, v_i) - A(\mu)u_i - B(\mu)v_i \\ g(\mu, u_i, v_i) - C(\mu)u_i - D(\mu)v_i \end{pmatrix}_{i=1}^{i=N}.$$

At $\mu = \mu_0$, system (2.8) reduces to

$$\frac{d\boldsymbol{U}}{dt} = \boldsymbol{M}(\mu_0)\boldsymbol{U} + \boldsymbol{F}_0(\boldsymbol{U}), \tag{2.10}$$

where $\boldsymbol{F}_0(\boldsymbol{U}) := \boldsymbol{F}(\mu, \boldsymbol{U})|_{\mu=\mu_0} = \boldsymbol{F}(\mu_0, \boldsymbol{U})$.

Let $\langle \cdot, \cdot \rangle$ be the complex-valued inner product on vector space $\mathbb{C}^{2N}$, defined as

$$\langle \boldsymbol{U}^{(1)}, \boldsymbol{U}^{(2)} \rangle = \sum_{i=1}^{N} \big(\bar{u}_i^{(1)} u_i^{(2)} + \bar{v}_i^{(1)} v_i^{(2)} \big), \tag{2.11}$$

where $\boldsymbol{U}^{(i)} = (u_1^{(i)}, v_1^{(i)}, \dots, u_N^{(i)}, v_N^{(i)}) \in \mathbb{C}^{2N}$ for i=1, 2. Clearly, $\langle \lambda \boldsymbol{U}^{(1)}, \boldsymbol{U}^{(2)} \rangle = \overline{\lambda} \langle \boldsymbol{U}^{(1)}, \boldsymbol{U}^{(2)} \rangle$. We denote the transposed matrix of $\boldsymbol{M}(\mu_0)$ as

$$\big(\boldsymbol{M}(\mu_0)\big)^T := \boldsymbol{I}_N \otimes \big(\boldsymbol{K}(\mu_0)\big)^T + \boldsymbol{L} \otimes \boldsymbol{D}. \tag{2.12}$$

From (H_1), we can then choose $\boldsymbol{q}^* := (a_n^* \phi_1^{(n)}, b_n^* \phi_1^{(n)}, \dots, \dots, a_n^* \phi_N^{(n)}, b_n^* \phi_N^{(n)})^T = \boldsymbol{\phi}^{(n)} \otimes \big(a_n^*, b_n^*\big)^T$ with $a_n^*, b_n^* \in \mathbb{C}$ satisfying $\big(\boldsymbol{M}_n(\mu_0)\big)^T \big(a_n^*, b_n^*\big)^T = -i\omega_0 \big(a_n^*, b_n^*\big)^T$ such that

$$\big(\boldsymbol{M}(\mu_0)\big)^T \boldsymbol{q}^* = -i\omega_0 \boldsymbol{q}^*, \quad \langle \boldsymbol{q}^*, \boldsymbol{q} \rangle = 1, \quad \text{and} \quad \langle \boldsymbol{q}^*, \bar{\boldsymbol{q}} \rangle = 0.$$

We can decompose $\mathbb{R}^{2N} = T^c \oplus T^{su}$ with $T^c := \{z\boldsymbol{q} + \bar{z}\bar{\boldsymbol{q}} | z \in \mathbb{C}\}$ and $T^{su} := \{\boldsymbol{U} \in X | \langle \boldsymbol{q}^*, \boldsymbol{U} \rangle = 0\}$. For any $\boldsymbol{U} = (u_1, v_1, \dots, u_N, v_N)^T$, there exists $z \in \mathbb{C}$ and $\boldsymbol{w} = (w_1^{(u)}, w_1^{(v)}, \dots, w_N^{(u)}, w_N^{(v)})^T \in T^{su}$ such that

$$\boldsymbol{U} = z\boldsymbol{q} + \bar{z}\bar{\boldsymbol{q}} + \boldsymbol{w}, \text{ or } \begin{cases} u_i = z a_n \phi_i^{(n)} + \bar{z} \cdot \overline{a_n} \phi_i^{(n)} + w_i^{(u)}, \\ v_i = z b_n \phi_i^{(n)} + \bar{z} \cdot \overline{b_n} \phi_i^{(n)} + w_i^{(v)}, \end{cases} \quad \text{for } i = 1, 2, \cdots, N. \tag{2.13}$$

Thus system (2.10) can be transformed to the following system in $(z, \boldsymbol{w})$ coordinates;

$$\begin{cases} \frac{dz}{dt} = i\omega_0 z + \langle \boldsymbol{q}^*, \boldsymbol{F}_0 \rangle, \\ \frac{d\boldsymbol{w}}{dt} = \boldsymbol{M}(\mu_0)\boldsymbol{w} + \boldsymbol{H}(z, \bar{z}, \boldsymbol{w}), \end{cases} \tag{2.14}$$

where

$$\boldsymbol{H}(z, \bar{z}, \boldsymbol{w}) := \boldsymbol{F}_0 - \langle \boldsymbol{q}^*, \boldsymbol{F}_0 \rangle \boldsymbol{q} - \langle \overline{\boldsymbol{q}^*}, \boldsymbol{F}_0 \rangle \bar{\boldsymbol{q}}, \quad \text{and} \quad \boldsymbol{F}_0 := \boldsymbol{F}_0(z\boldsymbol{q} + \bar{z}\bar{\boldsymbol{q}} + \boldsymbol{w}). \tag{2.15}$$

As in [22], we write $\boldsymbol{F}_0(\boldsymbol{U})$ in the form

$$\boldsymbol{F}_0(\boldsymbol{U}) := \frac{1}{2} Q(\boldsymbol{U}, \boldsymbol{U}) + \frac{1}{6} C(\boldsymbol{U}, \boldsymbol{U}, \boldsymbol{U}) + O(|\boldsymbol{U}|^4), \tag{2.16}$$

where $Q(\boldsymbol{X}, \boldsymbol{Y})$ and $C(\boldsymbol{X}, \boldsymbol{Y}, \boldsymbol{Z})$ are multilinear functions. In coordinates, we have

$$Q_i(\boldsymbol{X}, \boldsymbol{Y}) = \sum_{j,k=1}^{N} \frac{\partial^2 F_i(\boldsymbol{\xi})}{\partial \xi_j \partial \xi_k}\bigg|_{\boldsymbol{\xi}=\boldsymbol{0}} x_j y_k,$$

and

$$C_i(\boldsymbol{X}, \boldsymbol{Y}, \boldsymbol{Z}) = \sum_{j,k,l=1}^{N} \frac{\partial^3 F_i(\boldsymbol{\xi})}{\partial \xi_j \partial \xi_k \partial \xi_l}\bigg|_{\boldsymbol{\xi}=\boldsymbol{0}} x_j y_k z_l,$$

where $i = 1, 2, \dots, N$. For simplicity, we write $Q_{\boldsymbol{XY}} = Q(\boldsymbol{X}, \boldsymbol{Y})$, and $C_{\boldsymbol{XYZ}} = C(\boldsymbol{X}, \boldsymbol{Y}, \boldsymbol{Z})$. For later use, we calculate $Q_{\boldsymbol{qq}}$, $Q_{\boldsymbol{q}\bar{\boldsymbol{q}}}$ and $C_{\boldsymbol{qq}\bar{\boldsymbol{q}}}$ as follows:

$$\begin{aligned} Q_{\boldsymbol{qq}} &= \left(\cdots, (\phi_i^{(n)})^2 c_n, (\phi_i^{(n)})^2 d_n, \cdots\right)^T = \mathrm{col}\begin{pmatrix} (\phi_i^{(n)})^2 c_n \\ (\phi_i^{(n)})^2 d_n \end{pmatrix}_{i=1}^{i=N}, \\ Q_{\boldsymbol{q}\bar{\boldsymbol{q}}} &= \left(\cdots, (\phi_i^{(n)})^2 e_n, (\phi_i^{(n)})^2 f_n, \cdots\right)^T = \mathrm{col}\begin{pmatrix} (\phi_i^{(n)})^2 e_n \\ (\phi_i^{(n)})^2 f_n \end{pmatrix}_{i=1}^{i=N}, \\ C_{\boldsymbol{qq}\bar{\boldsymbol{q}}} &= \left(\cdots, (\phi_i^{(n)})^3 g_n, (\phi_i^{(n)})^3 h_n, \cdots\right)^T = \mathrm{col}\begin{pmatrix} (\phi_i^{(n)})^3 g_n \\ (\phi_i^{(n)})^3 h_n \end{pmatrix}_{i=1}^{i=N}, \end{aligned} \tag{2.17}$$

with

$$\begin{aligned} c_n &= f_{uu} a_n^2 + 2 f_{uv} a_n b_n + f_{vv} b_n^2, \\ d_n &= g_{uu} a_n^2 + 2 g_{uv} a_n b_n + g_{vv} b_n^2, \\ e_n &= f_{uu} |a_n|^2 + f_{uv}(a_n \overline{b_n} + \overline{a_n} b_n) + f_{vv} |b_n|^2, \\ f_n &= g_{uu} |a_n|^2 + g_{uv}(a_n \overline{b_n} + \overline{a_n} b_n) + g_{vv} |b_n|^2, \\ g_n &= f_{uuu} |a_n|^2 a_n + f_{uuv}(2|a_n|^2 b_n + a_n^2 \overline{b_n}) + f_{uvv}(2|b_n|^2 a_n + b_n^2 \overline{a_n}) + f_{vvv} |b_n|^2 b_n, \\ h_n &= g_{uuu} |a_n|^2 a_n + g_{uuv}(2|a_n|^2 b_n + a_n^2 \overline{b_n}) + g_{uvv}(2|b_n|^2 a_n + b_n^2 \overline{a_n}) + g_{vvv} |b_n|^2 b_n. \end{aligned} \tag{2.18}$$

Note that in (2.18), all partial derivatives are evaluated at $(\mu_0, 0, 0)$.

Let

$$\boldsymbol{H}(z, \bar{z}, \boldsymbol{w}) = \frac{\boldsymbol{H}_{20}}{2} z^2 + \boldsymbol{H}_{11} z \bar{z} + \frac{\boldsymbol{H}_{02}}{2} \bar{z}^2 + o(|z|^3) + o(|z| \cdot |\boldsymbol{w}|), \tag{2.19}$$

and note that

$$
\begin{aligned}
&\boldsymbol{H}(z,\overline{z},\boldsymbol{w})\\
&=\boldsymbol{F}_0-\langle\boldsymbol{q}^*,\boldsymbol{F}_0\rangle\boldsymbol{q}-\langle\overline{\boldsymbol{q}^*},\boldsymbol{F}_0\rangle\bar{\boldsymbol{q}}\\
&=\frac{1}{2}z^2\big(Q_{\boldsymbol{qq}}-\langle\boldsymbol{q}^*,Q_{\boldsymbol{qq}}\rangle\boldsymbol{q}-\langle\overline{\boldsymbol{q}^*},Q_{\boldsymbol{qq}}\rangle\bar{\boldsymbol{q}}\big)+z\overline{z}\big(Q_{\boldsymbol{q}\bar{\boldsymbol{q}}}-\langle\boldsymbol{q}^*,Q_{\boldsymbol{q}\bar{\boldsymbol{q}}}\rangle\boldsymbol{q}-\langle\overline{\boldsymbol{q}^*},Q_{\boldsymbol{q}\bar{\boldsymbol{q}}}\rangle\bar{\boldsymbol{q}}\big)\\
&\quad+\frac{1}{2}\overline{z}^2\big(Q_{\bar{\boldsymbol{q}}\bar{\boldsymbol{q}}}-\langle\boldsymbol{q}^*,Q_{\bar{\boldsymbol{q}}\bar{\boldsymbol{q}}}\rangle\boldsymbol{q}-\langle\overline{\boldsymbol{q}^*},Q_{\bar{\boldsymbol{q}}\bar{\boldsymbol{q}}}\rangle\bar{\boldsymbol{q}}\big)+\cdots,
\end{aligned}
$$

then matching the coefficients of terms z^2 and $z\overline{z}$ yields

$$
\begin{cases}\boldsymbol{H}_{20}=Q_{\boldsymbol{qq}}-\langle\boldsymbol{q}^*,Q_{\boldsymbol{qq}}\rangle\boldsymbol{q}-\langle\overline{\boldsymbol{q}^*},Q_{\boldsymbol{qq}}\rangle\bar{\boldsymbol{q}},\\ \boldsymbol{H}_{11}=Q_{\boldsymbol{q}\bar{\boldsymbol{q}}}-\langle\boldsymbol{q}^*,Q_{\boldsymbol{q}\bar{\boldsymbol{q}}}\rangle\boldsymbol{q}-\langle\overline{\boldsymbol{q}^*},Q_{\boldsymbol{q}\bar{\boldsymbol{q}}}\rangle\bar{\boldsymbol{q}},\end{cases}\tag{2.20}
$$

where

$$
\begin{aligned}
&\langle\boldsymbol{q}^*,Q_{\boldsymbol{qq}}\rangle=\big(\overline{a_n^*}c_n+\overline{b_n^*}d_n\big)\sum_{i=1}^N\big(\phi_i^{(n)}\big)^3,\quad \langle\overline{\boldsymbol{q}^*},Q_{\boldsymbol{qq}}\rangle=\big(a_n^*c_n+b_n^*d_n\big)\sum_{i=1}^N\big(\phi_i^{(n)}\big)^3,\\
&\langle\boldsymbol{q}^*,Q_{\boldsymbol{q}\bar{\boldsymbol{q}}}\rangle=\big(\overline{a_n^*}e_n+\overline{b_n^*}f_n\big)\sum_{i=1}^N\big(\phi_i^{(n)}\big)^3,\quad \langle\overline{\boldsymbol{q}^*},Q_{\boldsymbol{q}\bar{\boldsymbol{q}}}\rangle=\big(a_n^*e_n+b_n^*f_n\big)\sum_{i=1}^N\big(\phi_i^{(n)}\big)^3.
\end{aligned}
$$

It follows from Chapter 5 of [22] that system (2.14) possesses a center manifold, and then we can write $\boldsymbol{w}$ in the form

$$
\boldsymbol{w}=\frac{\boldsymbol{w}_{20}}{2}z^2+\boldsymbol{w}_{11}z\overline{z}+\frac{\boldsymbol{w}_{02}}{2}\overline{z}^2+o(|z|^3),\tag{2.21}
$$

where $\langle\boldsymbol{q}^*,\boldsymbol{w}_{ij}\rangle=0$, with $i,j=0,1,2,\ i+j=2$. By (2.19) and (2.21), together with

$$
\boldsymbol{M}(\mu_0)\boldsymbol{w}+\boldsymbol{H}(z,\overline{z},\boldsymbol{w})=\frac{d\boldsymbol{w}}{dt}=\frac{\partial\boldsymbol{w}}{\partial z}\cdot\frac{dz}{dt}+\frac{\partial\boldsymbol{w}}{\partial\overline{z}}\cdot\frac{d\overline{z}}{dt},
$$

we obtain

$$
\begin{cases}\boldsymbol{w}_{20}=[I_N\otimes(2i\omega_0I_2)-\boldsymbol{M}(\mu_0)]^{-1}\boldsymbol{H}_{20},\\ \boldsymbol{w}_{11}=-[\boldsymbol{M}(\mu_0)]^{-1}\boldsymbol{H}_{11},\end{cases}\tag{2.22}
$$

where $\boldsymbol{H}_{20}$ and $\boldsymbol{H}_{11}$ are given by (2.20).

Once we have $\boldsymbol{w}_{20}$ and $\boldsymbol{w}_{11}$, we can obtain the network-organized reaction-diffusion system restricted to the center manifold as

$$
\frac{dz}{dt}=i\omega_0z+\frac{1}{2}g_{20}z^2+g_{11}z\overline{z}+\frac{1}{2}g_{02}\overline{z}^2+\frac{1}{2}g_{21}z^2\overline{z}+O(|z|^4),\tag{2.23}
$$

where $g_{20}=\langle\boldsymbol{q}^*,Q_{\boldsymbol{qq}}\rangle$, $g_{11}=\langle\boldsymbol{q}^*,Q_{\boldsymbol{q}\bar{\boldsymbol{q}}}\rangle$, $g_{02}=\langle\boldsymbol{q}^*,Q_{\bar{\boldsymbol{q}}\bar{\boldsymbol{q}}}\rangle$, and

$$
g_{21}=2\langle\boldsymbol{q}^*,Q_{\boldsymbol{w}_{11}\boldsymbol{q}}\rangle+\langle\boldsymbol{q}^*,Q_{\boldsymbol{w}_{20}\bar{\boldsymbol{q}}}\rangle+\langle\boldsymbol{q}^*,C_{\boldsymbol{qq}\bar{\boldsymbol{q}}}\rangle.
$$

The dynamics of (2.14) could be determined by the dynamics of (2.23).

According to Chapter 3 of [22], we can write the *Poincaré* normal form of (2.8) (for μ in a neighborhood of μ_0) in the form

$$\frac{dz}{dt} = \big(\alpha(\mu) + i\omega(\mu)\big)z + z\sum_{j=1}^{M} c_j(\mu)(z\bar{z})^j, \tag{2.24}$$

where z is a complex variable, $M \geq 1$ and $c_j(\mu)$ are complex-valued coefficients. For $c_1(\mu)$, we have

$$c_1(\mu) = \frac{g_{20}g_{11}(3\alpha(\mu) + i\omega(\mu))}{2(\alpha^2(\mu) + \omega^2(\mu))} + \frac{|g_{11}|^2}{\alpha(\mu) + i\omega(\mu)} + \frac{|g_{02}|^2}{2(\alpha(\mu) + 3i\omega(\mu))} + \frac{g_{21}}{2}. \tag{2.25}$$

Thus, at $\mu = \mu_0$,

$$c_1(\mu_0) = \frac{i}{2\omega_0}\big(g_{20}g_{11} - 2|g_{11}|^2 - \frac{1}{3}|g_{02}|^2\big) + \frac{g_{21}}{2}. \tag{2.26}$$

Therefore, the real part of $c_1(\mu_0)$ is

$$\begin{aligned} \mathrm{Re}\big(c_1(\mu_0)\big) =& \mathrm{Re}\left(\frac{i}{2\omega_0}\langle \boldsymbol{q}^*, Q_{\boldsymbol{q}\boldsymbol{q}}\rangle \cdot \langle \boldsymbol{q}^*, Q_{\boldsymbol{q}\bar{\boldsymbol{q}}}\rangle\right) \\ &+ \mathrm{Re}\Big(\langle \boldsymbol{q}^*, Q_{\boldsymbol{w}_{11}\boldsymbol{q}}\rangle + \frac{1}{2}\langle \boldsymbol{q}^*, Q_{\boldsymbol{w}_{20}\bar{\boldsymbol{q}}}\rangle + \frac{1}{2}\langle \boldsymbol{q}^*, C_{\boldsymbol{q}\boldsymbol{q}\bar{\boldsymbol{q}}}\rangle\Big). \end{aligned} \tag{2.27}$$

To summarize the above analysis, we put forward the following Hopf bifurcation theorem for the general network-organized reaction-diffusion system (2.1).

Theorem 2.2. *Suppose* (H_1) *holds, then system* (2.1) *undergoes a Hopf bifurcation near the homogeneous equilibrium* E_{μ_0} *at* $\mu = \mu_0$. *Furthermore:*

1. *The bifurcation is supercritical (resp. subcritical) if* $\frac{1}{\alpha'(\mu_0)}Re(c_1(\mu_0)) < 0$ *(resp.* > 0*).*
2. *In addition, if all other eigenvalues of* $\boldsymbol{M}(\mu_0)$ *have negative real parts, then the bifurcating periodic solutions are stable (resp. unstable) if* $Re(c_1(\mu_0)) < 0$ *(resp.* > 0*).*

Remark 2.1. The above main theoretical result is similar to Theorem 2.1 in [39], and we emphasize some important points here.

1. As remarked in [39], we also note that under (H_1), if additionally there exists at least one eigenvalue of $\boldsymbol{M}(\mu_0)$ having positive real part, then the bifurcating periodic solutions are always unstable because the eigenvalues with positive real parts give rise to characteristic (Floquet) exponents with positive real parts.
2. For the class of ODEs taking forms as (2.1), $\mathrm{Re}(c_1(\mu_0))$ is difficult to be formulated in an explicit form. Formula (2.27) is just a form to compute $\mathrm{Re}(c_1(\mu_0))$. Indeed, in order to compute it, we first need to calculate $\langle \boldsymbol{q}^*, Q_{\boldsymbol{q}\boldsymbol{q}}\rangle$, $\langle \boldsymbol{q}^*, Q_{\boldsymbol{q}\bar{\boldsymbol{q}}}\rangle$, $\langle \boldsymbol{q}^*, Q_{\boldsymbol{w}_{11}\boldsymbol{q}}\rangle$, $\langle \boldsymbol{q}^*, Q_{\boldsymbol{w}_{20}\bar{\boldsymbol{q}}}\rangle$, and $\langle \boldsymbol{q}^*, C_{\boldsymbol{q}\boldsymbol{q}\bar{\boldsymbol{q}}}\rangle$. These terms are defined in other formulas as mentioned above, and substituting

these definitions into formula (2.27) will be lengthy. For concrete examples (like the one in the next section), we use (2.27) and corresponding substitutions to calculate these related quantities.

3. The last but not least, Theorem 2.1 is simple but indispensable in the derivation of the above result. This theorem provides us with a solid foundation to derive the considered Hopf bifurcation normal form. Actually, it can further guide us to investigate other bifurcation dynamics of the general or concrete network-organized reaction-diffusion systems.

Before ending this section, we would like to call for special attention to formula (2.20) of computing $\boldsymbol{H}_{20}$ and $\boldsymbol{H}_{11}$, and formula (2.22) of computing $\boldsymbol{\omega}_{20}$ and $\boldsymbol{\omega}_{11}$, which are quite different from the corresponding formulas (2.21), (2.24) and (2.27) in [39]. To show this important difference, we solve the solution of the following linear system as an illustration.

Lemma 2.1. *For a given $c_l \in \mathbb{C}$ which is not the eigenvalue of matrix $\boldsymbol{M}_l(\mu)$ where $\mu \in \mathbb{R}$, then for any $\big(a, b\big)^T \in \mathbb{R}^2$, the unique solution of the linear system*

$$\big[\boldsymbol{I}_N \otimes (c_l \boldsymbol{I}_2) - \boldsymbol{M}(\mu)\big]\left(\boldsymbol{\phi}^{(l)} \otimes \begin{pmatrix} x_1 \\ x_2 \end{pmatrix}\right) = \boldsymbol{\phi}^{(l)} \otimes \begin{pmatrix} a \\ b \end{pmatrix} \tag{2.28}$$

is given as

$$\begin{pmatrix} x_1 \\ x_2 \end{pmatrix} = \big[c_l \boldsymbol{I}_2 - \boldsymbol{M}_l(\mu)\big]^{-1} \begin{pmatrix} a \\ b \end{pmatrix},$$

for $l = 1, 2, \ldots, N$, where $\boldsymbol{M}(\mu)$ and $\boldsymbol{M}_l(\mu)$ are defined by (2.4) and (2.5) respectively, and Λ_l are Laplacian eigenvalues of network G with corresponding eigenvectors $\boldsymbol{\phi}^{(l)} = \big(\phi_1^{(l)}, \phi_2^{(l)}, \cdots, \phi_N^{(l)}\big)^T$, for $l = 1, 2, \ldots, N$.

Proof. Because $c_l \in \mathbb{C}$ is not the eigenvalue of matrix $\boldsymbol{M}_l(\mu)$, then by Theorem 2.1, $c_l \in \mathbb{C}$ is not the eigenvalue of matrix $\boldsymbol{M}(\mu)$ either. Therefore, (2.28) has a unique solution. Furthermore, it is straightforward to check that

$$\begin{aligned}
&\Big[\boldsymbol{I}_N \otimes (c_l \boldsymbol{I}_2) - \boldsymbol{M}(\mu)\Big]\left(\boldsymbol{\phi}^{(l)} \otimes \begin{pmatrix} x_1 \\ x_2 \end{pmatrix}\right) \\
&= \Big[\boldsymbol{I}_N \otimes (c_l \boldsymbol{I}_2) - \big(\boldsymbol{I}_N \otimes \boldsymbol{K}(\mu) + \boldsymbol{L} \otimes \boldsymbol{D}\big)\Big]\left(\boldsymbol{\phi}^{(l)} \otimes \begin{pmatrix} x_1 \\ x_2 \end{pmatrix}\right) \\
&= \Big[-\boldsymbol{L} \otimes \boldsymbol{D} + \boldsymbol{I}_N \otimes \big(c_l \boldsymbol{I}_2 - \boldsymbol{K}(\mu)\big)\Big]\left(\boldsymbol{\phi}^{(l)} \otimes \begin{pmatrix} x_1 \\ x_2 \end{pmatrix}\right) \\
&= -\big(\boldsymbol{L} \otimes \boldsymbol{D}\big)\left(\boldsymbol{\phi}^{(l)} \otimes \begin{pmatrix} x_1 \\ x_2 \end{pmatrix}\right) + \Big(\boldsymbol{I}_N \otimes \big(c_l \boldsymbol{I}_2 - \boldsymbol{K}(\mu)\big)\Big)\left(\boldsymbol{\phi}^{(l)} \otimes \begin{pmatrix} x_1 \\ x_2 \end{pmatrix}\right) \\
&= -\big(\boldsymbol{L}\boldsymbol{\phi}^{(l)}\big) \otimes \left(\boldsymbol{D}\begin{pmatrix} x_1 \\ x_2 \end{pmatrix}\right) + \big(\boldsymbol{I}_N \boldsymbol{\phi}^{(l)}\big) \otimes \left(\big(c_l \boldsymbol{I}_2 - \boldsymbol{K}(\mu)\big)\begin{pmatrix} x_1 \\ x_2 \end{pmatrix}\right) \\
&= -\big(\Lambda_l \boldsymbol{\phi}^{(l)}\big) \otimes \left(\boldsymbol{D}\begin{pmatrix} x_1 \\ x_2 \end{pmatrix}\right) + \boldsymbol{\phi}^{(l)} \otimes \left(\big(c_l \boldsymbol{I}_2 - \boldsymbol{K}(\mu)\big)\begin{pmatrix} x_1 \\ x_2 \end{pmatrix}\right)
\end{aligned}$$

$$= -\boldsymbol{\phi}^{(l)} \otimes \left(\Lambda_l \boldsymbol{D} \begin{pmatrix} x_1 \\ x_2 \end{pmatrix}\right) + \boldsymbol{\phi}^{(l)} \otimes \left(\left(c_l \boldsymbol{I}_2 - \boldsymbol{K}(\mu)\right) \begin{pmatrix} x_1 \\ x_2 \end{pmatrix}\right)$$

$$= \boldsymbol{\phi}^{(l)} \otimes \left(\left(c_l \boldsymbol{I}_2 - \boldsymbol{K}(\mu) - \Lambda_l \boldsymbol{D}\right) \begin{pmatrix} x_1 \\ x_2 \end{pmatrix}\right) = \boldsymbol{\phi}^{(l)} \otimes \left(\left(c_l \boldsymbol{I}_2 - \boldsymbol{M}_l(\mu)\right) \begin{pmatrix} x_1 \\ x_2 \end{pmatrix}\right).$$

Thus, due to (2.28), we have

$$\begin{pmatrix} x_1 \\ x_2 \end{pmatrix} = \left[c_l \boldsymbol{I}_2 - \boldsymbol{M}_l(\mu)\right]^{-1} \begin{pmatrix} a \\ b \end{pmatrix}.$$

Therefore, this lemma is proven. □

Based on formulas (2.20) and (2.22), and Lemma 2.1, we have the following comments:

Remark 2.2.

1. Given any underlying undirected network, the relation $\sum_{i=1}^{N} \left(\phi_i^{(n)}\right)^3 = 0$ does not surely hold for $n \neq 1$. By (2.20), then for $n \neq 1$, there are not surely $\boldsymbol{H}_{20} = \boldsymbol{Q}_{\boldsymbol{q}\boldsymbol{q}}$ or $\boldsymbol{H}_{11} = \boldsymbol{Q}_{\boldsymbol{q}\bar{\boldsymbol{q}}}$. This is different from the result that for $n \neq 0$, there are surely $\boldsymbol{H}_{20} = \boldsymbol{Q}_{\boldsymbol{q}\boldsymbol{q}}$ and $\boldsymbol{H}_{11} = \boldsymbol{Q}_{\boldsymbol{q}\bar{\boldsymbol{q}}}$ in [39].
2. Because there is not a universal relation similar to $\left(\phi_i^{(n)}\right)^2 = \left(\phi_i^{(2n)} + \phi_i^{(1)}\right)/2$ for $i = 1, 2, \dots, N$ and $n \neq 1$, like the special relation $\cos^2 \frac{n}{\ell} x = \left(\cos \frac{2n}{\ell} x + 1\right)/2$ used in PDE case in [39], the forms of $\boldsymbol{Q}_{\boldsymbol{q}\boldsymbol{q}}$ and $\boldsymbol{Q}_{\boldsymbol{q}\bar{\boldsymbol{q}}}$ given by (2.17) in (2.22) might not allow applying Lemma 2.1 to further compute $\boldsymbol{\omega}_{20}$ and $\boldsymbol{\omega}_{11}$ analytically. This situation may cause a big issue in computing $\mathrm{Re}(c_1(\mu_0))$, but we can handle this via numerical calculations.

3. Hopf bifurcation in a multi-patch predator-prey system

In this section, we provide an example to show the potential applicability of the above established theorem. To this end, we introduce a specific multi-patch predator-prey system.

We recall a homogeneous reaction-diffusion predator-prey model with the simplified dimensionless form as

$$\begin{cases} \frac{\partial}{\partial t} u(x,t) = D_u \Delta u(x,t) + u(1 - \frac{u}{k}) - \frac{muv}{1+u}, & x \in (0, \ell\pi), t > 0, \\ \frac{\partial}{\partial t} v(x,t) = D_v \Delta v(x,t) + \frac{muv}{1+u} - \theta v, & x \in (0, \ell\pi), t > 0, \\ u_x(0,t) = v_x(0,t) = 0, \quad u_x(\ell\pi, t) = v_x(\ell\pi, t) = 0, & t > 0, \\ u(x,0) = u_0(x) \geq 0, \quad v(x,0) = v_0(x) \geq 0, & x \in (0, \ell\pi), \end{cases} \tag{3.1}$$

where $u(x,t)$ and $v(x,t)$ represent the local dimensionless densities of the prey and predator at time $t \geq 0$ in a spatial position $x \in (0, \ell\pi)$ with $\ell \in \mathbb{R}^+$, respectively. This system has zero-flux boundary conditions and Holling type-II functional response. For the dimensionless parameters, k is the rescaled carrying capacity, θ is the death rate of the predator, m is the strength of the interaction, and D_u and D_v are the rescaled diffusion coefficients of the prey and predator, respectively. More details can be found in [39].

We consider the network analogue of system (3.1) as a specific example of (2.1). The network version of system (3.1) is written as

$$\begin{cases} \frac{d}{dt}u_i(t) = d_u \sum_{j=1}^{N} L_{ij}u_j + u_i(1 - \frac{u_i}{k}) - \frac{mu_i v_i}{1+u_i}, \\ \frac{d}{dt}v_i(t) = d_v \sum_{j=1}^{N} L_{ij}v_j + \frac{mu_i v_i}{1+u_i} - \theta v_i, \end{cases} \tag{3.2}$$

for $i = 1, 2, \ldots, N$, where u_i and v_i are local densities on node i of the prey and predator, respectively. We use d_u and d_v in system (3.2) to denote the diffusion coefficients of the prey and predator in discrete networks instead of D_u and D_v in system (3.1), since there does exist some difference in describing species diffusion in continuous space and discrete networks. Indeed, semidiscreting system (3.1) with meshing size h leads to one system (see system (3.42)), which is equivalent to one specified system of (3.2) defined on the non-periodic one-dimensional lattice network, where d_u and d_v equals D_u/h^2 and D_v/h^2 respectively.

For the corresponding ODE system of (3.1) or (3.2) without diffusion written in the following form

$$\begin{cases} \frac{d}{dt}u(t) = u(1 - \frac{u}{k}) - \frac{muv}{1+u}, \\ \frac{d}{dt}v(t) = \frac{muv}{1+u} - \theta v, \end{cases} \tag{3.3}$$

it is easy to find that system (3.3) always has the zero equilibrium $(0, 0)$ and a boundary equilibrium $(k, 0)$. It also has a coexistence equilibrium (μ, v_μ), where

$$\mu = \frac{\theta}{m - \theta}, \quad v_\mu = \frac{(k - \mu)(1 + \mu)}{km},$$

if and only if $m > \theta(1 + k)/k$ (or $0 < \mu < k$). Moreover, we shall recall the following stability information: if $\mu \geq k$, $(k, 0)$ is globally asymptotically stable; if $(k - 1)/2 < \mu < k$, (μ, v_μ) is globally asymptotically stable, while if $0 < \mu < (k - 1)/2$, there is a globally asymptotically stable periodic orbit. Especially, at $\mu = (k - 1)/2$, system (3.3) undergoes a subcritical Hopf bifurcation. See [20,39] and related references for more details.

Therefore, system (3.2) has only one positive homogeneous equilibrium $E_* : (u_i, v_i) = (\mu, v_\mu)$ for $i = 1, 2, \ldots, N$, provided $m > \theta(1 + k)/k$ (or $0 < \mu < k$). Of course, we are interested in analyzing the stability of E_* and further considering the related Hopf bifurcation for (3.2) defined on a certain underlying network G with fixed θ and k. We will use μ as the bifurcation parameter (or equivalently m as a parameter) as Yi et al. did in [39] for the convenience of direct comparison.

Setting $\widehat{u_i}(t) = u_i(t) - \mu$ and $\widehat{v_i}(t) = v_i(t) - v_\mu$ for $i = 1, 2, \ldots, N$, and then dropping the hats for simplification of notation, we have the transformed system:

$$\begin{cases} \frac{d}{dt}u_i(t) = d_u \sum_{j=1}^{N} L_{ij}u_j + (u_i + \mu)(1 - \frac{u_i+\mu}{k}) - \frac{m(u_i+\mu)(v_i+v_\mu)}{1+u_i+\mu}, \\ \frac{d}{dt}v_i(t) = d_v \sum_{j=1}^{N} L_{ij}v_j + \frac{m(u_i+\mu)(v_i+v_\mu)}{1+u_i+\mu} - \theta(v_i + v_\mu), \end{cases} \tag{3.4}$$

for $i = 1, 2, \ldots, N$. As in Section 2, we obtain the Jacobian matrix around $(u_i, v_i) = (0, 0)$ for $i = 1, 2, \ldots, N$ of system (3.4):

$$\boldsymbol{M}(\mu) = \boldsymbol{I}_N \otimes \boldsymbol{K}(\mu) + \boldsymbol{L} \otimes \boldsymbol{D}, \tag{3.5}$$

and the matrices in Theorem 2.1,

$$\boldsymbol{M}_l(\mu) = \boldsymbol{K}(\mu) + \Lambda_l \boldsymbol{D}, \tag{3.6}$$

where Λ_l are Laplacian eigenvalues for $l = 1, 2, \dots, N$, and

$$\boldsymbol{K}(\mu) = \begin{pmatrix} A(\mu) & B(\mu) \\ C(\mu) & D(\mu) \end{pmatrix}, \quad \boldsymbol{D} = \begin{pmatrix} d_u & 0 \\ 0 & d_v \end{pmatrix},$$

with $A(\mu) = \frac{\mu(k-1-2\mu)}{k(1+\mu)}$, $B(\mu) = -\theta$, $C(\mu) = \frac{k-\mu}{k(1+\mu)}$ and $D(\mu) = 0$.

The characteristic equation of $\boldsymbol{M}_l(\mu)$ is

$$\lambda^2 - \lambda T_l(\mu) + D_l(\mu) = 0, \quad l = 1, 2, \dots, N, \tag{3.7}$$

where

$$\begin{cases} T_l(\mu) = \frac{\mu(k-1-2\mu)}{k(1+\mu)} + (d_u + d_v)\Lambda_l, \\ D_l(\mu) = d_u d_v \Lambda_l^2 + \frac{d_v \mu(k-1-2\mu)}{k(1+\mu)} \Lambda_l + \theta \frac{k-\mu}{k(1+\mu)}. \end{cases} \tag{3.8}$$

We then identify the Hopf bifurcation value μ_0 that satisfies the condition (H_1) and is given as: There exists $n \in \{1, 2, \dots, N\}$ such that

$$T_n(\mu_0) = 0, \quad D_n(\mu_0) > 0, \quad \text{and} \quad T_l(\mu_0) \neq 0, \quad D_l(\mu_0) \neq 0, \quad \text{for} \quad l \neq n; \tag{3.9}$$

and for the unique pair of complex eigenvalues near the imaginary axis $\alpha(\mu) \pm i\omega(\mu)$,

$$\alpha'(\mu_0) \neq 0. \tag{3.10}$$

From (3.8), one can easily check that when $0 < k \leq 1$ or $k > 1$, but $(k-1)/2 < \mu < k$, $T_l(\mu) < 0$ and $D_l(\mu) > 0$ for $l = 1, 2, \dots, N$, which implies that the positive homogeneous equilibrium E_* is locally asymptotically stable. Therefore, we can state that any possible bifurcation point μ_0 must be in the interval $(0, (k-1)/2]$ with $k > 1$. For any possible Hopf bifurcation point μ_0 in $(0, (k-1)/2]$, $\alpha(\mu) \pm i\omega(\mu)$ are the eigenvalues of $\boldsymbol{M}_n(\mu)$, hence

$$\alpha(\mu) = \frac{T_n(\mu)}{2}, \quad \omega(\mu) = \sqrt{D_n(\mu) - \alpha(\mu)^2}, \tag{3.11}$$

and

$$\alpha'(\mu_0) = \frac{T_n'(\mu)}{2}\bigg|_{\mu=\mu_0} = \frac{k - 1 - 4\mu_0 - 2\mu_0^2}{2k(1+\mu_0)^2} \begin{cases} > 0, & \text{if } 0 < \mu_0 < \mu_*, \\ = 0, & \text{if } \mu_0 = \mu_*, \\ < 0, & \text{if } \mu_* < \mu_0 \leq (k-1)/2, \end{cases} \tag{3.12}$$

where

$$\mu_* = \sqrt{\frac{k+1}{2}} - 1 \in \left(0, \frac{k-1}{2}\right), \text{ with } k > 1. \tag{3.13}$$

Therefore, the transversality condition (3.10) is always satisfied as long as $\mu_0 \neq \mu_*$. From Theorem 2.1, we hence obtain that when $\mu_* < \mu_0 < (k-1)/2$, the real part of one pair of complex eigenvalues of $\boldsymbol{M}(\mu)$ becomes negative once μ increases crossing μ_0; and when $0 < \mu_0 < \mu_*$, the real part of one pair of complex eigenvalues of $\boldsymbol{M}(\mu)$ becomes positive once μ increases crossing μ_0.

Based on the above discussion, we can conclude that the determination of Hopf bifurcation points reduces to the description of the set

$$\begin{aligned}\mathbb{S}_H :=& \{\mu \in (0, \mu_*) \cup (\mu_*, (k-1)/2] : \\ & \text{for some } n \in \{1, 2, \ldots, N\},\ (3.9) \text{ and } (3.10) \text{ are satisfied}\},\end{aligned} \tag{3.14}$$

when a set of parameters (d_u, d_v, θ, k) and a certain underlying network G are provided.

In the following, we fix the underlying network G, parameters $\theta > 0$ and $k > 1$, and the ratio $\sigma = d_u/d_v$, but tune the value of d_v appropriately to determine the possible spatially homogeneous and nonhomogeneous Hopf bifurcation points of system (3.2). In our context, the bifurcating spatially homogeneous periodic solutions require that every node of the network exhibits homogeneous periodic dynamical behavior, while the bifurcating spatially nonhomogeneous periodic solutions admit that every node of the network exhibits nonhomogeneous periodic dynamical behavior.

We first consider the Hopf bifurcation of spatially homogeneous periodic solution of system (3.2). Actually, $\mu_1^H := (k-1)/2$ is always an element of $\mathbb{S}_H$, because $T_l(\mu_1^H) < T_1(\mu_1^H) = 0$ for $l = 2, 3, \ldots, N$, and $D_l(\mu_1^H) > 0$ for $l = 1, 2, \ldots, N$. Apparently, μ_1^H is the unique value μ for the Hopf bifurcation of spatially homogeneous periodic solution of system (3.2), which results from the fact that μ_1^H is the unique bifurcation point where its corresponding ODE system (3.3) undergoes the subcritical Hopf bifurcation.

We then seek the spatially nonhomogeneous Hopf bifurcation for $n \in \{2, 3, \ldots, N\}$. Note that $A(0) = A(\mu_1^H) = 0$, $A(\mu) > 0$ in $(0, \mu_1^H)$, and $A(\mu)$ has a unique critical point $\mu = \mu_*$ at which $A(\mu)$ takes a local maximum $A(\mu_*) = (\sqrt{k+1} - \sqrt{2})^2/k := M_* > 0$. We pick all single eigenvalues of the Laplacian matrix $\boldsymbol{L}$ of the given underlying network G as follows:

$$\mathbb{S}_{single} := \{\Lambda_{n_\tau} : 0 = \Lambda_1 = \Lambda_{n_1} > \Lambda_{n_2} > \cdots > \Lambda_{n_{M_1}}\}. \tag{3.15}$$

To consider the possible spatially nonhomogeneous Hopf bifurcation, we assume that the set $\mathbb{S}_{single}$ has at least two elements, equivalently $N \geq M_1 \geq 2$. Actually, this mild assumption is usually satisfied. Define

$$d_{v,\tau} := -\frac{M_*}{(1+\sigma)\Lambda_{n_\tau}}, \quad \tau = 2, \ldots, M_1. \tag{3.16}$$

Then for $d_{v,\tau+1} \leq d_v < d_{v,\tau}$, and $2 \leq j \leq \tau$, we define $\mu_{j,-}^H$ and $\mu_{j,+}^H$ to be the roots of $A(\mu) + (d_u + d_v)\Lambda_{n_j} = 0$ satisfying $0 < \mu_{j,-}^H < \mu_* < \mu_{j,+}^H < \mu_1^H$. All these points follow

$$0 < \mu_{2,-}^H < \mu_{3,-}^H < \cdots < \mu_{\tau,-}^H < \mu_* < \mu_{\tau,+}^H < \cdots < \mu_{3,+}^H < \mu_{2,+}^H < \mu_1^H.$$

Obviously, $T_{n_j}(\mu_{j,\pm}^H) = 0$ and $T_i(\mu_{j,\pm}^H) \neq 0$ for $i \neq n_j$. On the other hand, we also need to verify whether $D_i(\mu_{j,\pm}^H) \neq 0$ for $i = 1, 2, \ldots, N$, and in particular, $D_{n_j}(\mu_{j,\pm}^H) > 0$. Here, we just impose a sufficient condition so that $D_i(\mu) > 0$ for all $\mu \in [0, \mu_1^H]$, which implies $D_i(\mu_{j,\pm}^H) > 0$ for $i = 1, 2, \ldots, N$. Notice that the quadratic function $g(y) = d_u d_v y^2 + \frac{d_v \mu(k-1-2\mu)}{k(1+\mu)} y + \theta \frac{k-\mu}{k(1+\mu)}$ is positive for all $y \in \mathbb{R}$ if

$$\theta > \frac{d_v \mu^2 (k-1-2\mu)^2}{4 d_u k (k-\mu)(1+\mu)}.$$

Indeed, if $\mu \in [0, \mu_1^H]$, $\frac{1+\mu}{k-\mu} < 1$, then

$$\frac{d_v \mu^2 (k-1-2\mu)^2}{4 d_u k (k-\mu)(1+\mu)} = \frac{k d_v}{4 d_u} \cdot \frac{1+\mu}{(k-\mu)} \cdot \frac{\mu^2 (k-1-2\mu)^2}{k^2 (1+\mu) 2} < \frac{k d_v}{4 d_u} \cdot A^2(\mu) < \frac{k d_v M_*^2}{4 d_u}.$$

Therefore, if

$$\frac{\theta}{k} > \frac{d_v M_*^2}{4 d_u}, \tag{3.17}$$

then $D_i(\mu) > 0$ for $\mu \in [0, \mu_1^H]$, and particularly $D_i(\mu_{j,\pm}^H) > 0$ for $i = 1, 2, \ldots, N$.

Together with Theorem 2.2, we summarize the above analysis in the following theorem.

Theorem 3.1. *Given a certain underlying network G, and assume that the parameters $\theta > 0$, $k > 1$ and $m > \theta(1+k)/k$, and the ratio $\sigma = d_u/d_v$ satisfy*

$$\sigma = \frac{d_u}{d_v} > \frac{(\sqrt{k+1} - \sqrt{2})^4}{4\theta k}. \tag{3.18}$$

Then for any $d_v \in [d_{v,\tau+1}, d_{v,\tau})$ where $d_{v,\tau}$ are defined as in (3.16), there exist $2(\tau-1)$ points $\mu_{j,\pm}^H(G)$, $2 \leq j \leq \tau$, satisfying

$$0 < \mu_{2,-}^H(G) < \cdots < \mu_{\tau,-}^H(G) < \mu_* < \mu_{\tau,+}^H(G) < \cdots < \mu_{2,+}^H(G) < \mu_1^H,$$

such that the system (3.2) defined on network G undergoes a Hopf bifurcation at $\mu = \mu_{j,\pm}^H(G)$ or $\mu = \mu_1^H$. Moreover:

1. *The bifurcating periodic solutions from $\mu = \mu_1^H$ are spatially homogeneous, and they coincide with the periodic solutions of the corresponding ODE system;*
2. *The bifurcating periodic solutions from $\mu = \mu_{j,\pm}^H(G)$ are spatially nonhomogeneous.*

Remark 3.1.

1. Without the restriction (3.18), the system (3.2) defined on any connected undirected network always undergoes a Hopf bifurcation at $\mu = \mu_1^H$.
2. To make the condition (3.18) hold, (a) d_u/d_v should be large enough for any given $\theta > 0$ and $k > 1$; or (b) θ should be large enough while $k(> 1)$ small enough for any given $d_u, d_v > 0$. Meanwhile, (3.18) is actually a sufficient condition such that only Hopf bifurcations occur but steady state bifurcations do not occur. The latter possible bifurcations are not considered in this work. Of course, some Hopf bifurcations may still occur when (3.18) does not hold.
3. Introducing the set of single Laplacian eigenvalues $\mathbb{S}_{single}$ is necessary, since if there exists one multi Laplacian eigenvalue Λ_n such that $A(\mu) + (d_u + d_v)\Lambda_n = 0$, we might encounter other more intricate bifurcations. For example, if the Laplacian Λ_n of multiplicity 2 satisfying the condition $A(\mu)+(d_u+d_v)\Lambda_n = 0$, we need to deal with the double-Hopf bifurcation, which is not considered in this work. Note that this is quite different from the corresponding PDE case in [39], and suggests that the network may enrich the dynamical behaviors of system (3.2).
4. Take (3.18) into consideration again, with the fixed ratio $\sigma = d_u/d_v$ to make this condition hold for any given $\theta > 0$ and $k > 1$, we tune d_v such that $d_{v,\tau+1} \le d_v < d_{v,\tau}$ to allow the system having time-periodic spatially nonhomogeneous patterns. For the simplest case where Λ_2 is the largest single non-zero Laplacian eigenvalue, if $d_v \ge d_{v,2}$, then $\mu = \mu_1^H$ is the only Hopf bifurcation point, and $d_{v,2} := -M_*/(1+\sigma)/\Lambda_2$ is the maximal diffusion rate for the system to have a time-periodic spatial patterns. Moreover, smaller d_v usually implies more possible periodic spatially nonhomogeneous patterns. This revealed result is consistent with some ecological phenomena. Indeed, the sufficiently small diffusion rate of species will weaken the diffusion coupling and diminish the effect between nodes, which does lead to spatially nonhomogeneous distribution of populations. We finally would like to emphasize that different underlying networks usually have distinct Laplacian spectra, which can trigger substantial differences in their respective Hopf bifurcations. We will discuss this issue in detail in Section 4.

Next we consider the bifurcation direction and stability of the bifurcating spatially homogeneous periodic solutions.

Theorem 3.2. *For the system* (3.2) *defined on any underlying network G, the Hopf bifurcation at $\mu = \mu_1^H$ is subcritical, and the bifurcating spatially homogeneous periodic solutions are locally asymptotically stable.*

Proof. By Theorem 2.2, in order to determine the stability and bifurcation direction of the bifurcating periodic solution from $\mu = \mu_1^H$, we calculate $\mathrm{Re}(c_1(\mu_1^H))$. When $\mu = \mu_1^H$, we put

$$\begin{aligned} \boldsymbol{q} &= \boldsymbol{\phi}^{(1)} \otimes \begin{pmatrix} a_1 \\ b_1 \end{pmatrix} = \boldsymbol{\phi}^{(1)} \otimes \begin{pmatrix} 1 \\ -\frac{i\omega_1}{\theta} \end{pmatrix}, \\ \boldsymbol{q}^* &= \boldsymbol{\phi}^{(1)} \otimes \begin{pmatrix} a_1^* \\ b_1^* \end{pmatrix} = \boldsymbol{\phi}^{(1)} \otimes \begin{pmatrix} \frac{1}{2} \\ -\frac{i\theta}{2\omega_1} \end{pmatrix}, \end{aligned} \tag{3.19}$$

where $\omega_1 = \sqrt{\theta/k}$ and $\boldsymbol{\phi}^{(1)} = \left(1/\sqrt{N}, 1/\sqrt{N}, \dots, 1/\sqrt{N}\right)^T$.

In our context, we have

$$
\begin{aligned}
f(\mu,u,v) &= (u+\mu)(1-\frac{u+\mu}{k}) - \frac{m(u+\mu)(v+v_\mu)}{1+u+\mu},\\
g(\mu,u,v) &= \frac{m(u+\mu)(v+v_\mu)}{1+u+\mu} - \theta(v+v_\mu),
\end{aligned}
\tag{3.20}
$$

then we can compute all the following partial derivatives of f and g around $(\mu_1^H, 0, 0)$:

$$
\begin{aligned}
f_{uu} &= -\frac{2(k-1)}{k(k+1)}, \quad f_{uv} = -\frac{4\theta}{(k+1)(k-1)}, \quad f_{vv} = 0,\\
f_{uuu} &= -\frac{24}{k(1+k)^2}, \quad f_{uuv} = \frac{16\theta}{(k-1)(1+k)^2}, \quad f_{uvv} = f_{vvv} = 0,\\
g_{uu} &= -\frac{4}{k(1+k)}, \quad g_{uv} = \frac{4\theta}{(k+1)(k-1)}, \quad g_{vv} = 0,\\
g_{uuu} &= \frac{24}{k(1+k)^2}, \quad g_{uuv} = -\frac{16\theta}{(k-1)(1+k)^2}, \quad g_{uvv} = g_{vvv} = 0.
\end{aligned}
$$

By (2.18), we have

$$
\begin{aligned}
c_1 &= \frac{-2(k-1)^2 + 8i\omega_1 k}{k(k+1)(k-1)}, \quad d_1 = -\frac{4(k-1)+8i\omega_1 k}{k(k+1)(k-1)},\\
e_1 &= \frac{2(1-k)}{k(k+1)}, \quad f_1 = -\frac{4}{k(k+1)}, \quad g_1 = -h_1 = -\frac{24(k-1)+16i\omega_1 k}{k(k-1)(k+1)^2},
\end{aligned}
\tag{3.21}
$$

and

$$
\begin{aligned}
\langle \boldsymbol{q}^*, Q_{\boldsymbol{qq}}\rangle &= \frac{1}{\sqrt{N}} \cdot \frac{4\omega_1\theta k - (k-1)^2\omega_1 + 2\theta(3-k)i}{k(k-1)(k+1)\omega_1},\\
\langle \boldsymbol{q}^*, Q_{\boldsymbol{q}\bar{\boldsymbol{q}}}\rangle &= \frac{1}{\sqrt{N}} \cdot \frac{(1-k)\omega_1 - 2\theta i}{k(k+1)\omega_1},\\
\langle \overline{\boldsymbol{q}^*}, Q_{\boldsymbol{qq}}\rangle &= \frac{1}{\sqrt{N}} \cdot \frac{-(k-1)^2\omega_1 - 4\theta\omega_1 k + 2\theta(k+1)i}{k(k-1)(k+1)\omega_1},\\
\langle \overline{\boldsymbol{q}^*}, Q_{\boldsymbol{q}\bar{\boldsymbol{q}}}\rangle &= \frac{1}{\sqrt{N}} \cdot \frac{(1-k)\omega_1 + 2\theta i}{k(k+1)\omega_1},\\
\langle \boldsymbol{q}^*, C_{\boldsymbol{qq}\bar{\boldsymbol{q}}}\rangle &= \frac{1}{N} \cdot \frac{-12(k-1)\omega_1 - 8\theta\omega_1 k + 4(3k-5)\theta i}{k(k-1)(k+1)^2\omega_1}.
\end{aligned}
\tag{3.22}
$$

Therefore, it is straightforward to calculate

$$
\begin{aligned}
\boldsymbol{H}_{20} &= Q_{\boldsymbol{qq}} - \langle \boldsymbol{q}^*, Q_{\boldsymbol{qq}}\rangle \boldsymbol{q} - \langle \overline{\boldsymbol{q}^*}, Q_{\boldsymbol{qq}}\rangle \bar{\boldsymbol{q}} = \boldsymbol{0},\\
\boldsymbol{H}_{11} &= Q_{\boldsymbol{q}\bar{\boldsymbol{q}}} - \langle \boldsymbol{q}^*, Q_{\boldsymbol{q}\bar{\boldsymbol{q}}}\rangle \boldsymbol{q} - \langle \overline{\boldsymbol{q}^*}, Q_{\boldsymbol{q}\bar{\boldsymbol{q}}}\rangle \bar{\boldsymbol{q}} = \boldsymbol{0},
\end{aligned}
\tag{3.23}
$$

which implies that $\boldsymbol{w}_{20} = \boldsymbol{w}_{11} = \boldsymbol{0}$ from (2.22). Thus

$$\langle \boldsymbol{q}^*, Q_{\boldsymbol{w}_{11}\boldsymbol{q}} \rangle = \langle \boldsymbol{q}^*, Q_{\boldsymbol{w}_{20}\bar{\boldsymbol{q}}} \rangle = 0.$$

Therefore,

$$\begin{aligned}
\mathrm{Re}\,(c_1(\mu_0)) &= \mathrm{Re}\left\{ \frac{i}{2\omega_1} \langle \boldsymbol{q}^*, Q_{\boldsymbol{q}\boldsymbol{q}} \rangle \cdot \langle \boldsymbol{q}^*, Q_{\boldsymbol{q}\bar{\boldsymbol{q}}} \rangle + \frac{1}{2} \langle \boldsymbol{q}^*, C_{\boldsymbol{q}\boldsymbol{q}\bar{\boldsymbol{q}}} \rangle \right\} \\
&= \frac{\theta\big(4\theta k - (k-1)^2 - (3-k)(1-k)\big)}{Nk^2(k-1)(k+1)^2\omega_1^2} - \frac{6(k-1) + 4\theta k}{Nk(k-1)(k+1)^2} \\
&= \frac{4\theta k - (k-1)^2 - (3-k)(1-k)}{Nk(k-1)(k+1)^2} - \frac{6(k-1) + 4\theta k}{Nk(k-1)(k+1)^2} \\
&= \frac{4\theta k - (k-1)^2 - (3-k)(1-k) - 6(k-1) - 4\theta k}{Nk(k-1)(k+1)^2} \\
&= \frac{-2(k-1)(k+1)}{Nk(k-1)(k+1)^2} = -\frac{2}{Nk(k+1)} < 0.
\end{aligned} \tag{3.24}$$

From (3.12), it follows that $\alpha'(\mu_1^H) < 0$, and then by Theorem 2.2, the bifurcation is subcritical. On the other hand, from (3.8), $T_l(\mu_1^H) < 0$ and $D_l(\mu_1^H) > 0$ for $l = 2, 3, \ldots, N$, thus the bifurcating periodic solutions are stable since $\mathrm{Re}\,(c_1(\mu_0)) < 0$. $\square$

Then, for the spatially nonhomogeneous periodic solutions in Theorem 3.1, we have

Theorem 3.3. *For the system* (3.2) *defined on one certain underlying network G, the Hopf bifurcation at $\mu = \mu_{j,-}^H(G)$ is subcritical (supercritical) if $Re(c_1(\mu_{j,-}^H(G))) > 0(< 0)$, while the one at $\mu = \mu_{j,+}^H(G)$ is subcritical (supercritical) if $Re\big(c_1(\mu_{j,+}^H(G))\big) < 0(> 0)$, in which $Re(c_1(\mu_{j,\pm}^H(G)))$ is determined by* (3.31)*; and the bifurcating spatially nonhomogeneous periodic solutions are unstable.*

Proof. By (3.12), we have $\alpha'(\mu_{j,-}^H(G)) > 0$ and $\alpha'(\mu_{j,+}^H(G)) < 0$. To determine the bifurcation direction, we calculate $\mathrm{Re}(c_1(\mu_{j,\pm}^H(G)))$, with $\mu_{j,\pm}^H(G)$ satisfying the condition $A(\mu_{j,\pm}^H(G)) + (d_u + d_v)\Lambda_{n_j} = 0$.

When $\mu = \mu_{j,\pm}^H(G)$ with $2 \le j \le \tau$ and $2 \le n_j \le N$, we can set

$$\begin{aligned}
\boldsymbol{q} &= \boldsymbol{\phi}^{(n_j)} \otimes \begin{pmatrix} a_{n_j} \\ b_{n_j} \end{pmatrix} = \mathrm{col}\begin{pmatrix} a_{n_j}\phi_l^{(n_j)} \\ b_{n_j}\phi_l^{(n_j)} \end{pmatrix}_{l=1}^{l=N}, \\
\boldsymbol{q}^* &= \boldsymbol{\phi}^{(n_j)} \otimes \begin{pmatrix} a_{n_j}^* \\ b_{n_j}^* \end{pmatrix} = \mathrm{col}\begin{pmatrix} a_{n_j}^*\phi_l^{(n_j)} \\ b_{n_j}^*\phi_l^{(n_j)} \end{pmatrix}_{l=1}^{l=N},
\end{aligned} \tag{3.25}$$

where

$$
\begin{aligned}
a_{n_j} &= 1, \quad b_{n_j} = -\frac{d_v \Lambda_{n_j} + i\omega_{n_j}}{\theta}, \\
a^*_{n_j} &= \frac{\omega_{n_j} - i d_v \Lambda_{n_j}}{2\omega_{n_j}}, \quad b^*_{n_j} = -\frac{i\theta}{2\omega_{n_j}}, \\
\omega_{n_j} &= \sqrt{\theta C(\mu^H_{j,\pm}(G)) - d_v^2 \Lambda^2_{n_j}},
\end{aligned}
$$

and $\boldsymbol{\phi}^{(n_j)}$ is the normalized eigenvector of the network Laplacian matrix $\boldsymbol{L}$ with corresponding eigenvalue Λ_{n_j}.

We next compute the following partial derivatives of f and g evaluated at $(\mu^H_{j,\pm}(G), 0, 0)$:

$$
\begin{aligned}
f_{uu} &= \frac{-2\big(\mu^H_{j,\pm}(G)\big)^2 - 6\mu^H_{j,\pm}(G) + 2k - 2}{k\big(1+\mu^H_{j,\pm}(G)\big)^2}, \quad f_{uv} = -\frac{\theta}{\mu^H_{j,\pm}(G)\big(1+\mu^H_{j,\pm}(G)\big)}, \\
f_{uuu} &= -\frac{6\big(k-\mu^H_{j,\pm}(G)\big)}{k\big(1+\mu^H_{j,\pm}(G)\big)^3}, \quad f_{uuv} = \frac{2\theta}{\mu^H_{j,\pm}(G)\big(1+\mu^H_{j,\pm}(G)\big)^2}, \\
g_{uu} &= -\frac{2\big(k-\mu^H_{j,\pm}(G)\big)}{k\big(1+\mu^H_{j,\pm}(G)\big)^2}, \quad g_{uv} = \frac{\theta}{\mu^H_{j,\pm}(G)\big(1+\mu^H_{j,\pm}(G)\big)}, \\
g_{uuu} &= \frac{6\big(k-\mu^H_{j,\pm}(G)\big)}{k\big(1+\mu^H_{j,\pm}(G)\big)^3}, \quad g_{uuv} = -\frac{2\theta}{\mu^H_{j,\pm}(G)\big(1+\mu^H_{j,\pm}(G)\big)^2}, \\
f_{vv} &= f_{uvv} = f_{vvv} = 0, \quad g_{vv} = g_{uvv} = g_{vvv} = 0.
\end{aligned}
\tag{3.26}
$$

Then, (2.17) and (2.18) read as

$$
\begin{aligned}
Q_{\boldsymbol{qq}} &= \Big(\cdots, (\phi_l^{(n_j)})^2 c_{n_j}, (\phi_l^{(n_j)})^2 d_{n_j}, \cdots\Big)^T = \mathrm{col}\begin{pmatrix} (\phi_l^{(n_j)})^2 c_{n_j} \\ (\phi_l^{(n_j)})^2 d_{n_j} \end{pmatrix}_{l=1}^{l=N}, \\
Q_{\boldsymbol{q\bar{q}}} &= \Big(\cdots, (\phi_l^{(n_j)})^2 e_{n_j}, (\phi_l^{(n_j)})^2 f_{n_j}, \cdots\Big)^T = \mathrm{col}\begin{pmatrix} (\phi_l^{(n_j)})^2 e_{n_j} \\ (\phi_l^{(n_j)})^2 f_{n_j} \end{pmatrix}_{l=1}^{l=N}, \\
C_{\boldsymbol{qq\bar{q}}} &= \Big(\cdots, (\phi_l^{(n_j)})^3 g_{n_j}, (\phi_l^{(n_j)})^3 h_{n_j}, \cdots\Big)^T = \mathrm{col}\begin{pmatrix} (\phi_l^{(n_j)})^3 g_{n_j} \\ (\phi_l^{(n_j)})^3 h_{n_j} \end{pmatrix}_{l=1}^{l=N},
\end{aligned}
\tag{3.27}
$$

and

$$
\begin{aligned}
c_{n_j} &= f_{uu} - \frac{2d_v\Lambda_{n_j} + 2i\omega_{n_j}}{\theta} f_{uv}, \quad d_{n_j} = g_{uu} - \frac{2d_v\Lambda_{n_j} + 2i\omega_{n_j}}{\theta} g_{uv}, \\
e_{n_j} &= f_{uu} - \frac{2d_v\Lambda_{n_j}}{\theta} f_{uv}, \quad f_{n_j} = g_{uu} - \frac{2d_v\Lambda_{n_j}}{\theta} g_{uv}, \\
g_{n_j} &= f_{uuu} - \frac{3d_v\Lambda_{n_j} + i\omega_{n_j}}{\theta} f_{uuv}, \quad h_{n_j} = g_{uuu} - \frac{3d_v\Lambda_{n_j} + i\omega_{n_j}}{\theta} g_{uuv}.
\end{aligned}
\tag{3.28}
$$

By (2.20), we can obtain $\boldsymbol{H}_{20}$ and $\boldsymbol{H}_{11}$ as

$$\begin{aligned}\boldsymbol{H}_{20} &= Q_{\boldsymbol{q}\boldsymbol{q}} - \langle \boldsymbol{q}^*, Q_{\boldsymbol{q}\boldsymbol{q}}\rangle \boldsymbol{q} - \langle \overline{\boldsymbol{q}^*}, Q_{\boldsymbol{q}\boldsymbol{q}}\rangle \bar{\boldsymbol{q}},\\ \boldsymbol{H}_{11} &= Q_{\boldsymbol{q}\bar{\boldsymbol{q}}} - \langle \boldsymbol{q}^*, Q_{\boldsymbol{q}\bar{\boldsymbol{q}}}\rangle \boldsymbol{q} - \langle \overline{\boldsymbol{q}^*}, Q_{\boldsymbol{q}\bar{\boldsymbol{q}}}\rangle \bar{\boldsymbol{q}}.\end{aligned} \tag{3.29}$$

From (2.22), we obtain

$$\begin{cases}\boldsymbol{w}_{20} = [I_N \otimes (2i\omega_{n_j} I_2) - \boldsymbol{M}(\mu^H_{j,\pm}(G))]^{-1}\boldsymbol{H}_{20},\\ \boldsymbol{w}_{11} = -[\boldsymbol{M}(\mu^H_{j,\pm}(G))]^{-1}\boldsymbol{H}_{11},\end{cases} \tag{3.30}$$

where $\boldsymbol{H}_{20}$ and $\boldsymbol{H}_{11}$ are given by (3.29). Unfortunately, as we pointed out previously that the forms of $Q_{\boldsymbol{q}\boldsymbol{q}}$ and $Q_{\boldsymbol{q}\bar{\boldsymbol{q}}}$ in (3.27) might not allow applying Lemma 2.1 to further compute $\boldsymbol{\omega}_{20}$ and $\boldsymbol{\omega}_{11}$ analytically, which is different from the case in PDE where the special relation $\cos^2 \frac{n}{\ell}x = \left(\cos \frac{2n}{\ell}x + 1\right)/2$ holds such that we can obtain the analytic expressions for computing these terms. Therefore, (3.29) is just a form to compute $\boldsymbol{\omega}_{20}$ and $\boldsymbol{\omega}_{11}$.

By (2.27), we have

$$\begin{aligned}\mathrm{Re}\Big(c_1(\mu^H_{j,\pm}(G))\Big) =& \mathrm{Re}\Big(\frac{i}{2\omega_{n_j}}\langle \boldsymbol{q}^*, Q_{\boldsymbol{q}\boldsymbol{q}}\rangle \cdot \langle \boldsymbol{q}^*, Q_{\boldsymbol{q}\bar{\boldsymbol{q}}}\rangle\Big)\\ &+ \mathrm{Re}\Big(\langle \boldsymbol{q}^*, Q_{\boldsymbol{w}_{11}\boldsymbol{q}}\rangle\Big) + \frac{1}{2}\mathrm{Re}\Big(\langle \boldsymbol{q}^*, Q_{\boldsymbol{w}_{20}\bar{\boldsymbol{q}}}\rangle + \langle \boldsymbol{q}^*, C_{\boldsymbol{q}\boldsymbol{q}\bar{\boldsymbol{q}}}\rangle\Big).\end{aligned} \tag{3.31}$$

The bifurcating periodic solutions are unstable since the positive equilibrium E_* is unstable. In fact, for $1 \le i < n_j$, $T_i(\mu^H_{j,\pm}(G)) > T_{n_j}(\mu^H_{j,\pm}(G)) = 0$. Thereby, the bifurcating periodic solutions are unstable. □

We provide a special example by setting the underlying network in system (3.2) as the non-periodic one-dimensional lattice network of size N, $G_{la}(N)$. See an illustrative case where the network size is $N = 9$ in Fig. 1(a). There are two main reasons for considering this kind of networks. Firstly, we can find a similar relation like $\cos^2 \frac{n}{\ell}x = (\cos \frac{2n}{\ell}x + 1)/2$ to transform the expression of $Q_{\boldsymbol{q}\boldsymbol{q}}$ and $Q_{\boldsymbol{q}\bar{\boldsymbol{q}}}$, which allows applying Lemma 2.1 to further obtain an analytical expression to compute $\mathrm{Re}(c_1(\mu^H_{j,\pm}(G_{la})))$. Secondly, by introducing a spatially semidiscrete approximation to the continuous PDE system (3.1) using finite volume method, we can obtain this sample model as system (3.2) defined on G_{la} of the network size N. Such an example can bridge the occurrence and properties of the spatially nonhomogeneous periodic solutions in a network and in continuous space, and help distinguish their departures.

Following Liu et al. [24], we now introduce a spatially semidiscrete approximation to system (3.1) using finite volume method. Setting the meshing step size $h = \ell\pi/\widetilde{H}$ with $\widetilde{H} \in \mathbb{N}^+$, we get the mesh

$$\overline{\Omega}_h = \{x_l : x_l = lh, \quad l = 0, 1, 2, \dots, \widetilde{H}\}. \tag{3.32}$$

Letting $\Omega_l = [x_{l-\frac{1}{2}}, x_{l+\frac{1}{2}}]$ with $x_{l\pm\frac{1}{2}} = (l \pm \frac{1}{2})h$, and integrating the first equation of (3.1) on Ω_l leads to

$$\int_{\Omega_l} \frac{\partial u}{\partial t} dx = \int_{\Omega_l} f(u, v) dx + D_u \int_{\Omega_l} \frac{\partial^2 u}{\partial x^2} dx. \tag{3.33}$$

By mid-rectangle formula, the first two terms can be approximated as

$$\begin{aligned} I_1 &= \int_{\Omega_l} \frac{\partial u}{\partial t} dx = \int_{x_{l-\frac{1}{2}}}^{x_{l+\frac{1}{2}}} \frac{\partial u}{\partial t} dx \approx h \frac{du(x_l, t)}{dt}, \\ I_2 &= \int_{\Omega_l} f(u, v) dx = \int_{x_{l-\frac{1}{2}}}^{x_{l+\frac{1}{2}}} f(u, v) dx \approx h f\big(u(x_l, t), v(x_l, t)\big). \end{aligned} \tag{3.34}$$

For the third terms, from Newton-Leibniz formula and mid-rectangle formula, we have

$$\begin{aligned} I_3 &= D_u \int_{\Omega_l} \frac{\partial^2 u}{\partial x^2} dx = D_u \int_{x_{l-\frac{1}{2}}}^{x_{l+\frac{1}{2}}} \frac{\partial^2 u}{\partial x^2} dx \\ &= D_u \Big(\frac{\partial u(x_{l+\frac{1}{2}}, t)}{\partial x} - \frac{\partial u(x_{l-\frac{1}{2}}, t)}{\partial x} \Big) \\ &\approx \frac{D_u}{h} \Big[\big(u(x_{l+1}, t) - u(x_l, t) \big) - \big(u(x_l, t) - u(x_{l-1}, t) \big) \Big] \\ &= \frac{D_u}{h} \Big(u(x_{l+1}, t) - 2u(x_l, t) + u(x_{l-1}, t) \Big). \end{aligned} \tag{3.35}$$

By letting $u_l(t)$ be the finite volume approximation to $u(x_l, t)$, and according to (3.32) and (3.33)-(3.35), the spatially semidiscrete scheme for the first equation in (3.1) takes the following form

$$\frac{d}{dt} u_l(t) = f(u_l, v_l) + \frac{D_u}{h^2} \big(u_{l-1} - 2u_l + u_{l+1} \big). \tag{3.36}$$

Particularly, if x_l is a boundary node, such as x_0 and $x_{\widetilde{H}}$, it follows from (3.36) that

$$\begin{aligned} \frac{du_0}{dt} &= f(u_0, v_0) + \frac{D_u}{h^2} \big(u_{-1} - 2u_0 + u_1 \big), \\ \frac{du_{\widetilde{H}}}{dt} &= f(u_{\widetilde{H}}, v_{\widetilde{H}}) + \frac{D_u}{h^2} \big(u_{\widetilde{H}-1} - 2u_{\widetilde{H}} + u_{\widetilde{H}+1} \big). \end{aligned} \tag{3.37}$$

In the above formulas, the terms related to those nodes (or positions) x_{-1} and $x_{\widetilde{H}-1}$ outside $\overline{\Omega}_h$ can be eliminated by applying the zero-flux boundary conditions in (3.1). Note that the boundary condition of u is equivalent to

$$\frac{\partial}{\partial x} u_0(t) = \frac{\partial}{\partial x} u_{\widetilde{H}}(t) = 0. \tag{3.38}$$

Using Taylor expansion, we have

$$\begin{aligned} u_{-1}(t) &\approx u_0(t) - h\frac{\partial}{\partial x}u_0(t) = u_0(t), \\ u_{\widetilde{H}+1}(t) &\approx u_{\widetilde{H}}(t) + h\frac{\partial}{\partial x}u_{\widetilde{H}}(t) = u_{\widetilde{H}}(t). \end{aligned} \tag{3.39}$$

Thereby, for $u_0(t)$ and $u_{\widetilde{H}}(t)$, (3.37) can be written as

$$\begin{aligned} \frac{du_0}{dt} &= f(u_0, v_0) + \frac{D_u}{h^2}\big(-u_0 + u_1\big), \\ \frac{du_{\widetilde{H}}}{dt} &= f(u_{\widetilde{H}}, v_{\widetilde{H}}) + \frac{D_u}{h^2}\big(u_{\widetilde{H}-1} - u_{\widetilde{H}}\big). \end{aligned} \tag{3.40}$$

For the second equation in (3.1), we have a similar spatially semidiscrete approximation. Finally, by introducing the Laplacian matrix $\boldsymbol{L}$ of network G_{la} of size $N = \widetilde{H} + 1$ that takes the following form

$$\boldsymbol{L} = \begin{pmatrix} -1 & 1 & & & \\ 1 & -2 & 1 & & \\ & \ddots & \ddots & \ddots & \\ & & 1 & -2 & 1 \\ & & & 1 & -1 \end{pmatrix}, \tag{3.41}$$

we obtain the spatially semidiscrete approximating system of (3.1):

$$\begin{cases} \frac{d}{dt}u_i(t) = \frac{D_u}{h^2}\sum\limits_{j=1}^{N} L_{ij}u_j + u_i(1 - \frac{u_i}{k}) - \frac{mu_iv_i}{1+u_i}, \\ \frac{d}{dt}v_i(t) = \frac{D_v}{h^2}\sum\limits_{j=1}^{N} L_{ij}v_j + \frac{mu_iv_i}{1+u_i} - \theta v_i, \end{cases} \tag{3.42}$$

for $i = 1, 2, \ldots, N$, where L_{ij} are restricted as (3.41). Therefore, set $d_u = D_u/h^2$ and $d_v = D_v/h^2$, we obtain the corresponding system (3.2) defined on the non-periodic one-dimensional lattice network G_{la} of network size $N = \widetilde{H} + 1$.

Remark 3.2. The above spatially semidiscrete approximation to the continuous PDE system (3.1) is an indication that the spatiotemporal dynamics of the continuous PDE system (3.1) are limitedly supported in essence by the reaction-diffusion system (3.2) defined on the non-periodic one-dimensional lattice network G_{la}. In this sense, we would say that it is of urgent importance to investigate the reaction-diffusion system defined on various kinds of networks, even beyond this special kind of networks.

In the remaining part of this section, we always set the underlying network as the non-periodic one-dimensional lattice network $G_{la}(N)$. According to [26,21], the right normalized eigenvectors of Laplacian matrix $\boldsymbol{L}$ of network $G_{la}(N)$ are

$$\boldsymbol{\phi}^{(j)} = \sqrt{\frac{2}{N}}\left(\cos\tfrac{(j-1)\pi}{2N},\ \cos\tfrac{3(j-1)\pi}{2N},\ \ldots,\ \cos\tfrac{(2N-1)(j-1)\pi}{2N}\right)^T, \tag{3.43}$$

with corresponding eigenvalues $\Lambda_j = 2\cos\frac{(j-1)\pi}{N} - 2$, for $j = 2, 3, \ldots, N$. In addition, when $j = 1$, the eigenvalue is $\Lambda_1 = 0$ with the corresponding normalized eigenvector

$$\boldsymbol{\phi}^{(1)} = \left(1/\sqrt{N},\ 1/\sqrt{N},\ \ldots,\ 1/\sqrt{N}\right)^T.$$

Therefore, we can particularly obtain the set

$$\mathbb{S}_{single} := \{\Lambda_n : 0 = \Lambda_1 > \Lambda_2 > \cdots > \Lambda_N\}. \tag{3.44}$$

According to Theorem 3.1, we are able to obtain the following corollary.

Corollary 3.1. *Set the underlying network as the non-periodic one-dimensional lattice network of size N, i.e. $G_{la}(N)$, and assume that the parameters $\theta > 0$, $k > 1$ and $m > \theta(1+k)/k$, and especially, $d_u = D_u/h^2$ and $d_v = D_v/h^2$ with D_u, $D_v > 0$ and $h = \ell\pi/(N-1)$ where $\ell \in \mathbb{R}^+$ satisfy*

$$\frac{d_u}{d_v} = \frac{D_u}{D_v} > \frac{(\sqrt{k+1}-\sqrt{2})^4}{4\theta k}. \tag{3.45}$$

Then, for any $\ell \in (\ell_n, \ell_{n+1}]$ with

$$\ell_n := \frac{N-1}{\pi}\sqrt{\frac{-(D_u+D_v)}{M_*}\left(2\cos\frac{(n-1)\pi}{N} - 2\right)} \tag{3.46}$$

for $n = 2, 3, \ldots, N$, there exist $2(n-1)$ points $\mu^H_{j,\pm}(G_{la})$ determined by $A(\mu) + (d_u + d_v)\Lambda_n = A(\mu) + 2(d_u + d_v)\left(\cos\frac{(n-1)\pi}{N} - 1\right) = 0$ for $j = 2, 3, \ldots, n$, satisfying

$$0 < \mu^H_{2,-}(G_{la}) < \cdots < \mu^H_{n,-}(G_{la}) < \mu_* < \mu^H_{n,+}(G_{la}) < \cdots < \mu^H_{2,+}(G_{la}) < \mu^H_1,$$

such that the system (3.2) defined on the network $G_{la}(N)$ undergoes a Hopf bifurcation at $\mu = \mu^H_{j,\pm}(G_{la})$ or $\mu = \mu^H_1$. Moreover:

1. *The bifurcating periodic solutions from $\mu = \mu^H_1$ are spatially homogeneous, and they coincide with the periodic solutions of the corresponding ODE system;*
2. *The bifurcating periodic solutions from $\mu = \mu^H_{j,\pm}(G_{la})$ are spatially nonhomogeneous.*

One can similarly put forward a series of comments like Remark 3.1, but here we only would like to highlight something important.

Remark 3.3.

1. It is easy to check $\lim\limits_{N\to+\infty} \ell_n = \lim\limits_{N\to+\infty} \frac{N-1}{\pi}\sqrt{\frac{-(D_u+D_v)}{M_*}\left(2\cos\frac{(n-1)\pi}{N} - 2\right)} = (n-1)\sqrt{\frac{D_u+D_v}{M_*}}$ for $n = 2, 3, \ldots$, which is totally in line with equation (2.47) in [39] by transforming their index starting from 2. Actually, taking account for the case where N takes $+\infty$, the occur-

rence of Hopf bifurcations of system (3.2) defined on the network G_{la} is of no difference from the results of the PDE system (3.1) revealed by Theorem 2.4 in [39].

2. With all Laplacian eigenvalues of network G_{la} being single, $\mu = \mu_1^H$ is the only Hopf bifurcation point if $0 < \ell < \ell_2$, where

$$\ell_2 = \frac{N-1}{\pi}\sqrt{\frac{-(D_u+D_v)}{M_*}\left(2\cos\frac{\pi}{N}-2\right)}.$$

As in [39], this fact means that $\ell_2\pi$ is a minimal lattice length for the system to have a time-periodic spatial pattern. For this minimal lattice length $\ell_2\pi$, it is worth putting out that $\ell_2\pi$ grows with a limit

$$\lim_{N\to+\infty} \ell_2\pi = \frac{\pi\sqrt{(d_u+d_v)k}}{\sqrt{k+1}-\sqrt{2}}$$

as we increase the network size N to $+\infty$. Besides, we should pay attention to the fact that more periodic patterns are possibly triggered by increasing lattice length $\ell\pi$. In our consideration, increasing lattice length $\ell\pi$ or decreasing network size N does mean equivalently tuning the diffusion rates d_u and d_v smaller, which is essential to induce heterogeneous distribution of populations. In this spirit, the minimal lattice length $\ell_2\pi$ makes the same ecological sense to our previously discussed maximal diffusion rate $d_{v,2}$. At the same time, once we increase the network size N, we also need to enlarge the lattice length $\ell\pi$ appropriately to keep the sufficiently small diffusion rates and thereby result in the time-periodic spatial heterogeneity in the system.

3. In system (3.2) defined on other types of networks instead of the network G_{la}, we can also set $d_u = D_u/h^2$ and $d_v = D_v/h^2$ with $D_u,\ D_v > 0$ and $h = \ell\pi/(N-1)$ where $\ell \in \mathbb{R}^+$ by ignoring the influence of the edge length (the distance between the connected nodes) on species diffusion rates. Then we can also define the characteristic length as

$$\ell_n := \frac{N-1}{\pi}\sqrt{\frac{-(D_u+D_v)}{M_*}\Lambda_n}, \tag{3.47}$$

for $n = 2, 3, \ldots, N$. Following the same logic in Corollary 3.1, we can similarly discuss the corresponding Hopf bifurcations of the system (3.2) defined on the non-periodic one-dimensional lattice network. We will show some applications in our Examples 4.2-4.4 in Section 4.

Without any doubt, Theorem 3.2 supports that the system (3.2) defined on network G_{la} undergoes a subcritical Hopf bifurcation, and the bifurcating spatially homogeneous periodic solutions are locally asymptotically stable.

For the bifurcation direction and stability of the bifurcating spatially nonhomogeneous solutions, we can state the following theorem.

Theorem 3.4. *For the system* (3.2) *defined on the non-periodic one-dimensional lattice network* G_{la}*, the Hopf bifurcation at* $\mu = \mu_{j,-}^H(G_{la})$ *is subcritical (supercritical) if* $Re(c_1(\mu_{j,-}^H(G_{la}))) > 0 (< 0)$*, while the one at* $\mu = \mu_{j,+}^H(G_{la})$ *is subcritical (supercritical) if* $Re(c_1(\mu_{j,+}^H(G_{la}))) < 0 (>$

0), *in which* $Re(c_1(\mu^H_{j,\pm}(G_{la})))$ *is determined by* (A.23), (A.24) *and* (A.25)*; and furthermore, the bifurcating spatially nonhomogeneous periodic solutions are unstable.*

Proof. It is clear that the bifurcating periodic solutions are unstable since the positive equilibrium E_* is unstable. In fact, for $1 \le i < j$, $T_i(\mu^H_{j,\pm}(G)) > T_j(\mu^H_{j,\pm}(G)) = 0$. Thereby, the bifurcating periodic solutions are unstable. The bifurcation direction is determined by (3.12) and Theorem 2.2. The calculation of $\mathrm{Re}(c_1(\mu^H_{j,\pm}(G_{la})))$, given by (A.23), (A.24) and (A.25), is lengthy, and we provide the details in Appendix A. Together with $\alpha'(\mu^H_{j,-}(G_{la})) > 0$ and $\alpha'(\mu^H_{j,+}(G_{la})) < 0$ from (3.12), we obtain that, for the system (3.2) defined on the special underlying network G_{la}, the Hopf bifurcation at $\mu = \mu^H_{j,-}(G_{la})$ is subcritical (supercritical) if $\mathrm{Re}(c_1(\mu^H_{j,-}(G_{la}))) > 0 (< 0)$, while the one at $\mu = \mu^H_{j,+}(G_{la})$ is subcritical (supercritical) if $\mathrm{Re}(c_1(\mu^H_{j,+}(G_{la}))) < 0 (> 0)$. $\square$

Remark 3.4. In the above theorem, the procedure of calculating $\mathrm{Re}(c_1(\mu^H_{j,\pm}(G_{la})))$ shown in Appendix A is very similar to the corresponding procedure in Appendix A of [39]. However, our obtained formulas of $\mathrm{Re}(c_1(\mu^H_{j,\pm}(G_{la})))$ are quite different.

4. Numerical simulations

In this section, we provide some illustrative numerical simulations for system (3.2) defined on several typical networks to confirm our theoretical results obtained in Section 3, and more importantly, to investigate the effects of each underlying network on Hopf bifurcations.

We briefly introduce the following four kinds of networks to be used as the candidate underlying networks.

- **The non-periodic one-dimensional lattice network**. In this network, all nodes are placed into a one-dimensional lattice with the non-periodic boundary conditions, and each is connected with its possible nearest neighbors on its left and right by undirected edges. That is, each inner node is connected with one adjacent node on its left and right; and the right (left) boundary node is connected with its one left (right) adjacent node. For convenience, we denote $G_{la}(N)$ as the non-periodic one-dimensional lattice network composed of N nodes. See the illustrative network $G_{la}(9)$ in Fig. 1(a).
- **The non-periodic one-dimensional K-nearest lattice network**. In this network, all nodes are also placed into a one-dimensional lattice with the non-periodic boundary conditions, but each is connected with its all possible K nearest neighbors on its left and right by undirected edges. We here denote $G_n(N, K)$ as the non-periodic one-dimensional K-nearest lattice network of size N. Clearly, once $K = 1$, the non-periodic one-dimensional 1-nearest lattice network $G_n(N, 1)$ reduces to the non-periodic one-dimensional lattice network $G_{la}(N)$. See the illustrative network $G_n(9, 2)$ in Fig. 1(b).
- **The non-periodic one-dimensional small-world lattice network**. We perform a random rewiring procedure to a prepared non-periodic one-dimensional K-nearest lattice network to generate this network. Concretely, for each edge in the prepared non-periodic one-dimensional K-nearest lattice network, we break it with a given probability $P \in [0, 1]$ and reconnect one of its two ending nodes chosen with equal probability to a node chosen uniformly at random over the entire lattice, with duplicate edges forbidden; otherwise we leave

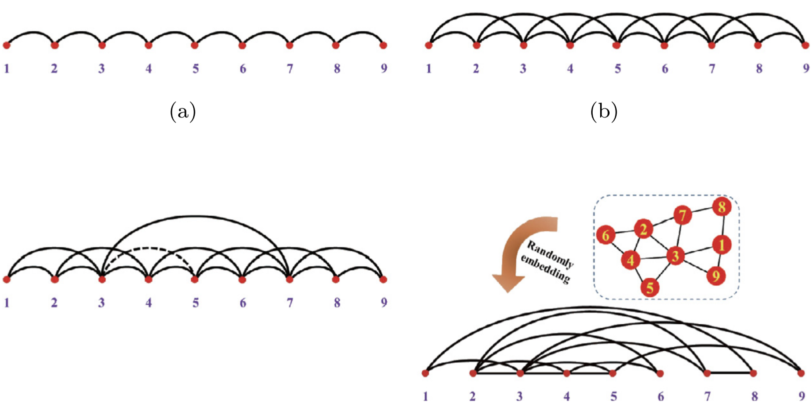

(a) (b) (c) (d)

Fig. 1. Illustrative networks: (a) the non-periodic one-dimensional lattice network $G_{la}(9)$, (b) the non-periodic one-dimensional 2-nearest lattice network $G_n(9, 2)$, (c) the non-periodic one-dimensional small-world lattice network $G_{sw}(9, 2, 0.1)$, in which the dash arc connecting node 3 and 5 is the broken edge, and the long arc connecting node 3 and node 7 is the rewired edge, (d) the randomly embedded one-dimensional scale-free lattice network $G_{sf}(9, 2)$, whose corresponding Barabási-Albert scale-free network before randomly embedding is inside the dash rectangle.

the edge in place. Here, the generated network is denoted by $G_{sw}(N, K, P)$. Note that when $P = 0$, the network $G_{sw}(N, K, P)$ reduces to the network $G_n(N, K)$. See the illustrative network $G_{sw}(9, 2, 0.1)$ in Fig. 1(c) where there exists only one random rewiring edge.

- **The randomly embedded one-dimensional scale-free lattice network**. To generate this network, we first generate one Barabási-Albert scale-free network by the preferential attachment algorithm [3], in which m new connections are added at each iteration step. Then, we randomly place each node into a distinct site to occupy all sites of a one-dimensional lattice for randomly embedding the network. We denote $G_{sf}(N, \widetilde{m})$ as the randomly embedded one-dimensional scale-free lattice network of size N with parameter $\widetilde{m}$. See the illustrative network $G_{sf}(9, 2)$ in Fig. 1(d).

After setting up the four types of candidate underlying networks, we provide our examples for system (3.2) defined on different underlying networks. It is conceivable that we work on different underlying networks under the same other parameters in our examples. As in [39], we choose $k = 17$, $\theta = 4$, $d_u = D_u/h^2$ and $d_v = D_v/h^2$ with $D_u = 1$, $D_v = 3$, $h = \ell\pi/199$ where $\ell = 2\sqrt{119}/7$ or $\ell = 4\sqrt{85}/5$. Direct computation shows that $\mu_1^H = 8$, $\mu_* = 2$, $M_* = 8/17$, and condition (3.18) is satisfied. Especially, the first example considers the system (3.2) defined on the non-periodic one-dimensional lattice network. This example serves as a counterpart for the PDE system (3.1) provided in [39], and shall play as a baseline to compare the results in other three examples. By distinguishing the differences between these results, we finally can infer and conclude some effects of the underlying networks on Hopf bifurcations.

Example 4.1. Set the underlying network as the non-periodic one-dimensional lattice network of size $N = 200$, i.e., $G_{la}(200)$, whose single Laplacian eigenvalues are $\Lambda_n = 2\cos\frac{(n-1)\pi}{200} - 2$ for $n = 1, 2, \ldots, N$. Therefore, by (3.46), we have $\ell_n = \frac{199}{\pi}\sqrt{17(1 - \cos\frac{(n-1)\pi}{200})}$ for $n = 2, 3, \ldots, N$. Particularly, $\Lambda_2 \approx -0.000247$, $\Lambda_3 \approx -0.000987$ and $\Lambda_4 \approx -0.002220$, and correspondingly $\ell_2 \approx 2.900867$, $\ell_3 \approx 5.801559$ and $\ell_4 \approx 8.701890$. Therefore, we have the following results:

1. Let $\ell = 2\sqrt{119}/7 \approx 3.116775$, then $\ell \in (\ell_2, \ell_3] \approx (2.900867, 5.801559]$. Solving $A(\mu) + 2(d_u + d_v)(\cos\frac{\pi}{200} - 1) = 0$, we have $\mu_{2,-}^H \approx 0.972693$ and $\mu_{2,+}^H \approx 3.562290$. Then, we obtain the set of Hopf bifurcation points

$$\mathbb{S}_H = \{\mu_{2,-}^H, \mu_{2,+}^H, \mu_1^H\} \approx \{0.972693, 3.562290, 8\}.$$

By the computation of (A.23), we have $\mathrm{Re}(\mu_{2,-}^H) \approx -0.003217 < 0$, $\mathrm{Re}(\mu_{2,+}^H) \approx -0.000197 < 0$, and by (3.12), we have $\alpha'(\mu_{2,-}^H) > 0$ and $\alpha'(\mu_{2,+}^H) < 0$. Therefore, the bifurcation direction is supercritical and subcritical at $\mu = \mu_{2,-}^H$ and $\mu = \mu_{2,+}^H$ respectively;
2. Let $\ell = 4\sqrt{85}/5 \approx 7.375636$, then $\ell \in (\ell_3, \ell_4] \approx (5.801559, 8.701890]$. Solving $A(\mu) + 2(d_u + d_v)(\cos\frac{\pi}{200} - 1) = 0$, we have $\mu_{2,-}^H \approx 0.084802$ and $\mu_{2,+}^H \approx 7.296445$. And, solving $A(\mu) + 2(d_u + d_v)(\cos\frac{\pi}{100} - 1) = 0$, we have $\mu_{3,-}^H \approx 0.491682$ and $\mu_{3,+}^H \approx 5.033460$. Then, we obtain the set of Hopf bifurcation points

$$\mathbb{S}_H = \{\mu_{2,-}^H, \mu_{3,-}^H, \mu_{3,+}^H, \mu_{2,+}^H, \mu_1^H\} \approx \{0.084802, 0.491682, 5.033460, 7.296445, 8\}.$$

By the computation of (A.23), we have $\mathrm{Re}(\mu_{2,-}^H) \approx -0.110655 < 0$, $\mathrm{Re}(\mu_{3,-}^H) \approx -0.010671 < 0$, $\mathrm{Re}(\mu_{3,+}^H) \approx -0.000090 < 0$ and $\mathrm{Re}(\mu_{2,+}^H) \approx -0.000049 < 0$, and by (3.12), we have $\alpha'(\mu_{2,-}^H) > 0$ and $\alpha'(\mu_{3,-}^H) > 0$, $\alpha'(\mu_{3,+}^H) < 0$ and $\alpha'(\mu_{2,+}^H) < 0$. Therefore, the bifurcation direction is supercritical at $\mu = \mu_{2,-}^H$ and $\mu = \mu_{3,-}^H$; and subcritical at $\mu = \mu_{2,+}^H$ and $\mu = \mu_{3,+}^H$.

Example 4.2. Set the underlying network as the non-periodic one-dimensional 2-nearest lattice network of size $N = 200$, i.e., $G_n(200, 2)$, whose first two largest non-zero single Laplacian eigenvalues are $\Lambda_2 \approx -0.001234$ and $\Lambda_3 \approx -0.004933$. By (3.47), we have $\ell_2 \approx 6.486374$ and $\ell_3 \approx 12.971358$. Therefore, we have the following results:

1. Let $\ell = 2\sqrt{119}/7 \approx 3.116775$, then $\ell < \ell_2 \approx 6.486374$. Thereby, there exists only one Hopf bifurcation point $\mu = \mu_1^H$;
2. Let $\ell = 4\sqrt{85}/5 \approx 7.375636$, then $\ell \in (\ell_2, \ell_3] \approx (6.486374, 12.971358]$. Solving $A(\mu) + (d_u + d_v)\Lambda_2 = 0$, we have $\mu_{2,-}^H \approx 0.743060$ and $\mu_{2,+}^H \approx 4.163332$. Then, we obtain the set of Hopf bifurcation points

$$\mathbb{S}_H = \{\mu_{2,-}^H, \mu_{2,+}^H, \mu_1^H\} \approx \{0.743060, 4.163332, 8\}.$$

By the computation of (A.23), we have $\mathrm{Re}(\mu_{2,-}^H) \approx -0.005294 < 0$, $\mathrm{Re}(\mu_{2,+}^H) \approx -0.000111 < 0$, and by (3.12), we have $\alpha'(\mu_{2,-}^H) > 0$ and $\alpha'(\mu_{2,+}^H) < 0$. Therefore, the bifurcation direction is supercritical and subcritical at $\mu = \mu_{2,-}^H$ and $\mu = \mu_{2,+}^H$ respectively.

Example 4.3. Set the underlying network as $G_{sw}(200, 2, 0.05)$, whose largest non-zero single Laplacian eigenvalue is $\Lambda_2 \approx -0.042189$. By (3.47), we have $\ell_2 \approx 37.932611$. Therefore, we have the following results:

1. Let $\ell = 2\sqrt{119}/7 \approx 3.116775$, then $\ell < \ell_2 \approx 37.932611$. Thereby, there exists only one Hopf bifurcation point $\mu = \mu_1^H$;
2. Let $\ell = 4\sqrt{85}/5 \approx 7.375636$, then $\ell < \ell_2 \approx 37.932611$. Thereby, there exists only one Hopf bifurcation point $\mu = \mu_1^H$ as well.

Example 4.4. Set the underlying network as $G_{sf}(200, 2)$, whose largest non-zero single Laplacian eigenvalue is $\Lambda_2 \approx -0.581614$. By (3.47), we have $\ell_2 \approx 140.841275$. Therefore, we have the following results:

1. Let $\ell = 2\sqrt{119}/7 \approx 3.116775$, then $\ell < \ell_2 \approx 140.841275$. Thereby, there exists only one Hopf bifurcation point $\mu = \mu_1^H$;
2. Let $\ell = 4\sqrt{85}/5 \approx 7.375636$, then $\ell < \ell_2 \approx 140.841275$. Thereby, there exists only one Hopf bifurcation point $\mu = \mu_1^H$ as well.

In the above four examples, one can find that increasing the parameter K in network $G_n(N, K)$ or the parameter P in network $G_{sw}(N, K, P)$ will hinder the emergence of the bifurcating nonhomogeneous periodic solutions. The same consequence also lies in network $G_{sf}(N, \widetilde{m})$. To explain this difference, we should pay attention to the decreasing Laplacian eigenvalues (especially including Λ_2 and Λ_3) from Example 4.1 to Example 4.4. From a mathematical point of view, we can conclude that the decrement of Laplacian eigenvalues requires larger ℓ (smaller diffusion rate of species) to keep the emergence of bifurcating nonhomogeneous periodic solutions.

More importantly, we would like to understand these results with apparent distinctiveness from an ecological perspective. Actually, increasing the parameter K in network $G_n(N, K)$ does increase the number of diffusion routines of each node to its nearest nodes (landscape patches) in networks, which allows the prey and predators move among more patches on a larger scale. As a result, this enhancement of diffusion coupling would suppress the heterogeneous spatial distribution of individuals.

In the network $G_{sw}(N, K, P)$, the rewired edges play a role as some stochastic routines between nodes in network to mimic the random movement of populations. The sufficiently more rewired edges with increasing P will lead to the phenomenon of “small world”. The shorter average (path) length makes the effect of each node better transmitted to the nodes of the whole network directly or indirectly, especially including the nodes which are far apart in the one-dimensional lattice space. In the ecological perspective, the stochastic routines would promote spatial homogeneity of population distribution.

Example 4.4 shows the disappearance of Hopf bifurcation for spatially nonhomogeneous periodic solutions, which might result from the existence of hubs in the Barabási-Albert scale-free network. Imagine that the hub nodes play as some centers in a network to connect with a large number of nodes, and strengthen the effect between all nodes in a network even indirectly. This important centrality induces the spatially homogeneous dynamical behaviors of populations.

According to the above results, we finally provide a group of numerical simulations to show the bifurcating unstable spatially nonhomogeneous periodic solution of prey for system (3.2) defined on the network $G_{la}(200)$ in Fig. 2, and the network $G_n(200, 2)$ in Fig. 3, the corresponding bifurcating stable spatially homogeneous periodic solution of prey for system (3.2) defined on network $G_{sw}(200, 2, 0.05)$ in Fig. 4, and the network $G_{sf}(200, 2)$ in Fig. 5. In these simulations, we set the same parameters as $N = 200$, $k = 17$, $\theta = 4$, $\mu = 4$, $d_u = D_u/h^2$ and $d_v = D_v/h^2$ with $D_u = 1$, $D_v = 3$, $h = \ell\pi/199$ where $\ell = 4\sqrt{85}/5$, and the same initial condi-

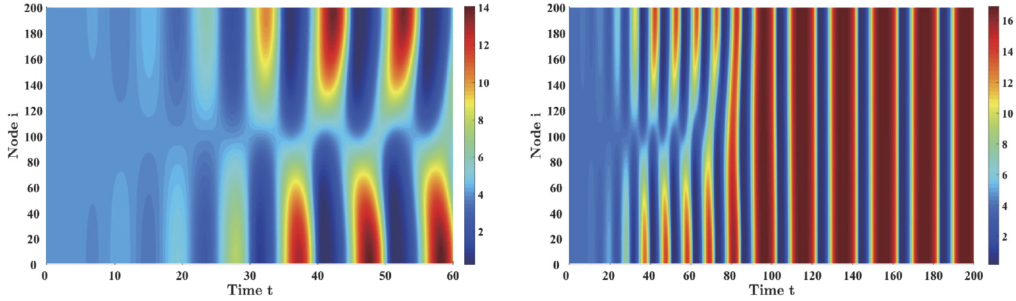

(a) (b)

Fig. 2. The bifurcating unstable spatially nonhomogeneous periodic solution of system (3.2) defined on network $G_{la}(200)$.

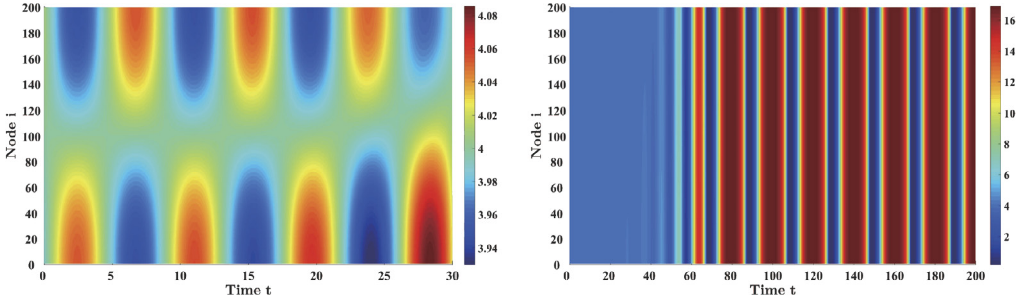

(a) (b)

Fig. 3. The bifurcating unstable spatially nonhomogeneous periodic solution of system (3.2) defined on network $G_n(200, 2)$.

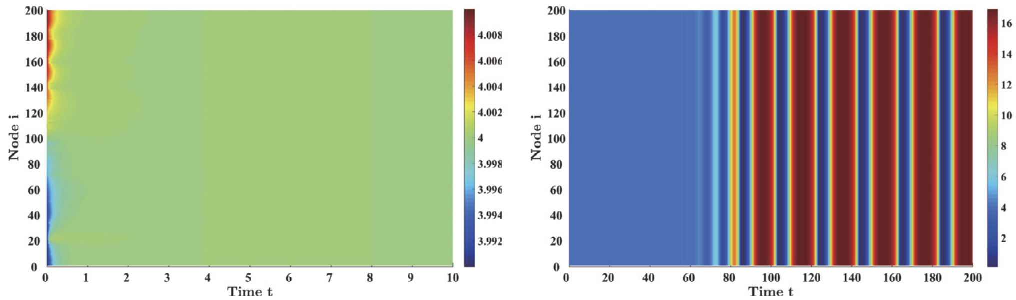

(a) (b)

Fig. 4. The bifurcating stable spatially homogeneous periodic solution of system (3.2) defined on network $G_{sw}(200, 2, 0.05)$.

tions as $u_i(0) = 4 - 0.01\cos\big((2i-1)\pi/400\big)$, $v_i(0) = 0.764709 - 0.01\cos\big((2i-1)\pi/400\big)$ for $i = 1, 2, \ldots, 200$.

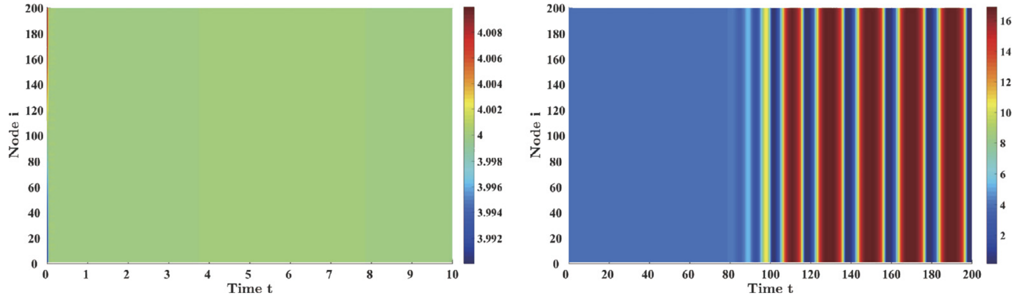

(a) (b)

Fig. 5. The bifurcating stable spatially homogeneous periodic solution of system (3.2) defined on network $G_{sf}(200, 2)$.

5. Discussion

In this paper, with the aid of Kronecker product, we demonstrated the fundamental Theorem 2.1, and then rigorously established the Hopf bifurcation Theorem 2.2 for the general homogeneous network-organized reaction-diffusion systems. Our Hopf bifurcation theorem can be extended to the delayed network-organized reaction-diffusion systems, where the delay needs to be incorporated cautiously.

We further provided a rigorous exploration for the Hopf bifurcation in a multi-patch predator-prey system (3.2), which can be defined on any underlying network. The foremost point to mention is that the studied system (3.2) defined on the non-periodic one-dimensional lattice network can be viewed as one spatially semidiscrete approximating system of the corresponding reaction-diffusion system subject to Neumann boundary conditions on one-dimensional spatial domain, with a necessary rescaling of the diffusion rates. As expected, its results about Hopf bifurcations were in good agreement with those of the corresponding PDE system. Like Yi et al. [39], we could determine a minimum lattice length $\ell\pi$ depending on the network size N for the existence of time-periodic spatially nonhomogeneous solutions as well. Moreover, we demonstrated that more possible periodic patterns could be triggered by increasing lattice length $\ell\pi$. More importantly, we could derive the analytic expressions for computing quantity $\mathrm{Re}(c_1(\mu_0))$ of its bifurcating spatially nonhomogeneous periodic solutions, even though they were of different forms.

By considering the system (3.2) defined on any connected undirected network, including the non-periodic one-dimensional lattice networks, with the fixed ratio $\sigma = d_u/d_v$ satisfying the condition (3.18), we found that there existed a maximal diffusion rate of d_v (and d_u concurrently) for the system to possess a bifurcating spatially nonhomogeneous periodic solution. In addition, decreasing the diffusion rate might induce more bifurcating spatially nonhomogeneous periodic solutions. Since increasing ℓ meant decreasing the diffusion rates with the fixed ratio $\sigma = d_u/d_v$, these conclusions were in the same spirit of the statement about the lattice length $\ell\pi$ in the last paragraph. These results might support an ecological observation that the sufficiently small diffusion rate of species will weaken the coupling and diminish the effect between patches, which can lead to spatially nonhomogeneous distribution of populations.

When system (3.2) was defined on other underlying networks, rather than the special non-periodic one-dimensional lattice network, more differences exhibited. This was mainly due to the Laplacian spectrum of different underlying networks. Mathematically it was difficult to get the analytic expressions for computing quantity $\mathrm{Re}(c_1(\mu_0))$ of its bifurcating spatially nonhomogeneous periodic solutions, without the support of Lemma 2.1. On the other hand, as we showed in the four examples in Section 4, when the largest single negative Laplacian eigenvalue Λ_2 decreased, the number of the possible spatially nonhomogeneous Hopf bifurcation points decreased and could even become zero. In our examples, the causes of this phenomenon may include more edges to nodal farther nearest neighbors on a nonlocal scale, sufficient rewired stochastic edges, and the emergence of hub nodes with large connectivity. These results could lead to some new ecological laws. The enhanced coupling between nodes by the increasing nonlocal connected edges would suppress the heterogeneous spatial distribution of individuals. The phenomenon of "small world" triggered by randomly rewired edges might make each node better transmitted to the nodes of the whole network directly or indirectly, and promote spatial homogeneity of population distribution. Furthermore, the hub nodes in a network could play as some centers that strengthen the effect between nodes and lead to the spatially homogeneous dynamical behaviors.

One missing part in this study is that we only consider the periodic solutions bifurcating from the single Laplacian eigenvalue, but do not study the possible periodic solutions bifurcating from multiple eigenvalues. Further analysis of the Hopf bifurcation in the reaction-diffusion system defined on the directed underlying networks remains a challenging problem. Hopefully our fundamental Theorem 2.1 will stimulate more research on rigorous bifurcation analysis in the general or some concrete reaction-diffusion systems defined on networks.

Acknowledgments

This work is supported by the National Natural Science Foundation of China under grant 61873154 and the Natural Sciences and Engineering Research Council of Canada under Individual discovery grant RGPIN-2020-03911 and Discovery Accelerator Supplement Award RGPAS-2020-00090.

Appendix A. The calculation of $\mathrm{Re}(c_1(\mu^H_{j,\pm}(G_{la})))$ in Theorem 3.4

In this appendix, we provide the lengthy calculation of $\mathrm{Re}(c_1(\mu^H_{j,\pm}(G_{la})))$ in Theorem 3.4. As a necessary preparation, we first state one important relation about the normalized eigenvectors of Laplacian matrix (3.41) of the non-periodic one-dimensional lattice network. Based on (3.43), we denote

$$(\boldsymbol{\phi}_{\cdot}^{(j)})^2 := \frac{2}{N}\left(\cos^2\frac{(j-1)\pi}{2N},\ \cos^2\frac{3(j-1)\pi}{2N},\ \ldots,\ \cos^2\frac{(2N-1)(j-1)\pi}{2N}\right)^T,$$

then, when N is odd, we have

$$(\boldsymbol{\phi}_{\cdot}^{(j)})^2 = \begin{cases} \frac{1}{\sqrt{2N}}\boldsymbol{\phi}^{(2j-1)} + \frac{1}{\sqrt{N}}\boldsymbol{\phi}^{(1)}, & 2 \le j \le \frac{N+1}{2}, \\ -\frac{1}{\sqrt{2N}}\boldsymbol{\phi}^{(2(N+2-j)-1)} + \frac{1}{\sqrt{N}}\boldsymbol{\phi}^{(1)}, & \frac{N+3}{2} \le j \le N, \end{cases} \tag{A.1}$$

and when N is even, we have

$$\left(\boldsymbol{\phi}_{\cdot}^{(j)}\right)^2 = \begin{cases} \frac{1}{\sqrt{2N}}\boldsymbol{\phi}^{(2j-1)} + \frac{1}{\sqrt{N}}\boldsymbol{\phi}^{(1)}, & 2 \le j \le \frac{N}{2}, \\ \frac{1}{\sqrt{N}}\boldsymbol{\phi}^{(1)}, & j = \frac{N}{2}+1, \\ -\frac{1}{\sqrt{2N}}\boldsymbol{\phi}^{(2(N+2-j)-1)} + \frac{1}{\sqrt{N}}\boldsymbol{\phi}^{(1)}, & \frac{N}{2}+1 < j \le N. \end{cases} \tag{A.2}$$

Then, we consider the case where N is odd for calculating $\mathrm{Re}(c_1(\mu_{j,\pm}^H(G_{la})))$, in which $\mu_{j,\pm}^H(G_{la})$ satisfies the following condition

$$A(\mu_{j,\pm}^H(G_{la})) + 2(d_u + d_v)\big(\cos\frac{(j-1)\pi}{N} - 1\big) = 0.$$

For the other case where N is even, $\mathrm{Re}(c_1(\mu_{j,\pm}^H(G_{la})))$ can be obtained in a similar way.

When $\mu = \mu_{j,\pm}^H(G_{la})$ with $2 \le j \le N$, we can set

$$\begin{aligned} \boldsymbol{q} &= \boldsymbol{\phi}^{(j)} \otimes \begin{pmatrix} a_j \\ b_j \end{pmatrix} = \mathrm{col}\begin{pmatrix} \phi_l^{(j)} a_j \\ \phi_l^{(j)} b_j \end{pmatrix}_{l=1}^{l=N}, \\ \boldsymbol{q}^* &= \boldsymbol{\phi}^{(j)} \otimes \begin{pmatrix} a_j^* \\ b_j^* \end{pmatrix} = \mathrm{col}\begin{pmatrix} \phi_l^{(j)} a_j^* \\ \phi_l^{(j)} b_j^* \end{pmatrix}_{l=1}^{l=N}, \end{aligned} \tag{A.3}$$

where

$$\begin{aligned} & a_j = 1, \quad b_j = -\frac{2d_v(\cos\frac{(j-1)\pi}{N} - 1) + i\omega_j}{\theta}, \\ & a_j^* = \frac{\omega_j - 2id_v(\cos\frac{(j-1)\pi}{N} - 1)}{2\omega_j}, \quad b_j^* = -\frac{i\theta}{2\omega_j}, \\ & \omega_j = \sqrt{\theta C\big(\mu_{j,\pm}^H(G_{la})\big) - 4d_v^2\Big(\cos\frac{(j-1)\pi}{N} - 1\Big)^2}, \\ & \boldsymbol{\phi}^{(j)} = \sqrt{\frac{2}{N}}\left(\cos\tfrac{(j-1)\pi}{2N},\ \cos\tfrac{3(j-1)\pi}{2N},\ \ldots,\ \cos\tfrac{(2N-1)(j-1)\pi}{2N}\right)^T. \end{aligned}$$

We next compute the following partial derivatives of f and g evaluated at $\big(\mu_{j,\pm}^H(G_{la}), 0, 0\big)$:

$$
\begin{aligned}
f_{uu} &= \frac{-2\big(\mu^H_{j,\pm}(G_{la})\big)^2 - 6\mu^H_{j,\pm}(G_{la}) + 2k - 2}{k\big(1+\mu^H_{j,\pm}(G_{la})\big)^2}, \quad f_{uv} = -\frac{\theta}{\mu^H_{j,\pm}(G_{la})\big(1+\mu^H_{j,\pm}(G_{la})\big)}, \\
f_{uuu} &= -\frac{6\big(k-\mu^H_{j,\pm}(G_{la})\big)}{k\big(1+\mu^H_{j,\pm}(G_{la})\big)^3}, \quad f_{uuv} = \frac{2\theta}{\mu^H_{j,\pm}(G_{la})\big(1+\mu^H_{j,\pm}(G_{la})\big)^2}, \\
g_{uu} &= -\frac{2\big(k-\mu^H_{j,\pm}(G_{la})\big)}{k\big(1+\mu^H_{j,\pm}(G_{la})\big)^2}, \quad g_{uv} = \frac{\theta}{\mu^H_{j,\pm}(G_{la})\big(1+\mu^H_{j,\pm}(G_{la})\big)}, \\
g_{uuu} &= \frac{6\big(k-\mu^H_{j,\pm}(G_{la})\big)}{k\big(1+\mu^H_{j,\pm}(G_{la})\big)^3}, \quad g_{uuv} = -\frac{2\theta}{\mu^H_{j,\pm}(G_{la})\big(1+\mu^H_{j,\pm}(G_{la})\big)^2}, \\
f_{vv} &= f_{uvv} = f_{vvv} = 0, \quad g_{vv} = g_{uvv} = g_{vvv} = 0.
\end{aligned}
\tag{A.4}
$$

Then, (2.17) and (2.18) read as

$$
\begin{aligned}
Q_{\boldsymbol{qq}} &= \left(\cdots, c_j \cos^2\frac{(2i-1)(j-1)\pi}{2N}, d_j \cos^2\frac{(2i-1)(j-1)\pi}{2N}, \cdots\right)^T \\
&= \mathrm{col}\begin{pmatrix} c_j \cos^2\frac{(2i-1)(j-1)\pi}{2N} \\ d_j \cos^2\frac{(2i-1)(j-1)\pi}{2N} \end{pmatrix}_{i=1}^{i=N}, \\
Q_{\boldsymbol{q\bar{q}}} &= \left(\cdots, e_j \cos^2\frac{(2i-1)(j-1)\pi}{2N}, f_j \cos^2\frac{(2i-1)(j-1)\pi}{2N}, \cdots\right)^T \\
&= \mathrm{col}\begin{pmatrix} e_j \cos^2\frac{(2i-1)(j-1)\pi}{2N} \\ f_j \cos^2\frac{(2i-1)(j-1)\pi}{2N} \end{pmatrix}_{i=1}^{i=N}, \\
C_{\boldsymbol{qq\bar{q}}} &= \left(\cdots, g_j \cos^3\frac{(2i-1)(j-1)\pi}{2N}, h_j \cos^3\frac{(2i-1)(j-1)\pi}{2N}, \cdots\right)^T \\
&= \mathrm{col}\begin{pmatrix} g_j \cos^3\frac{(2i-1)(j-1)\pi}{2N} \\ h_j \cos^3\frac{(2i-1)(j-1)\pi}{2N} \end{pmatrix}_{i=1}^{i=N},
\end{aligned}
\tag{A.5}
$$

and

$$
\begin{aligned}
c_j &= f_{uu} + P_1 f_{uv} + iP_2 f_{uv}, \quad d_j = g_{uu} + P_1 g_{uv} + iP_2 g_{uv}, \\
e_j &= f_{uu} + P_1 f_{uv}, \quad f_j = g_{uu} + P_1 g_{uv}, \\
g_j &= f_{uuu} + \frac{3}{2}P_1 f_{uuv} + \frac{i}{2}P_2 f_{uuv}, \\
h_j &= g_{uuu} + \frac{3}{2}P_1 g_{uuv} + \frac{i}{2}P_2 g_{uuv},
\end{aligned}
\tag{A.6}
$$

with

$$
P_1 = -\frac{4d_v\big(\cos\frac{(j-1)\pi}{N} - 1\big)}{\theta}, \quad \text{and} \quad P_2 = -\frac{2\omega_j}{\theta}. \tag{A.7}
$$

In this case, due to $\sum_{i=1}^{N}\left(\phi_i^{(j)}\right)^3=0$ for $j=2,3,\ldots,N$, we have $\langle \boldsymbol{q}^*, Q_{\boldsymbol{qq}}\rangle = \langle \boldsymbol{q}^*, Q_{\boldsymbol{q}\bar{\boldsymbol{q}}}\rangle = 0$. Thus $\boldsymbol{H}_{20}=Q_{\boldsymbol{qq}}$ and $\boldsymbol{H}_{11}=Q_{\boldsymbol{q}\bar{\boldsymbol{q}}}$. In fact, together with (A.1), we obtain that when N is odd,

$$\boldsymbol{H}_{20}=\begin{cases}\frac{1}{\sqrt{2N}}\boldsymbol{\phi}^{(2j-1)}\otimes\begin{pmatrix}c_j\\ d_j\end{pmatrix}+\frac{1}{\sqrt{N}}\boldsymbol{\phi}^{(1)}\otimes\begin{pmatrix}c_j\\ d_j\end{pmatrix}, & 2\le j\le \frac{N+1}{2},\\ -\frac{1}{\sqrt{2N}}\boldsymbol{\phi}^{(2(N+2-j)-1)}\otimes\begin{pmatrix}c_j\\ d_j\end{pmatrix}+\frac{1}{\sqrt{N}}\boldsymbol{\phi}^{(1)}\otimes\begin{pmatrix}c_j\\ d_j\end{pmatrix}, & \frac{N+3}{2}\le j\le N,\end{cases} \tag{A.8}$$

and

$$\boldsymbol{H}_{11}=\begin{cases}\frac{1}{\sqrt{2N}}\boldsymbol{\phi}^{(2j-1)}\otimes\begin{pmatrix}e_j\\ f_j\end{pmatrix}+\frac{1}{\sqrt{N}}\boldsymbol{\phi}^{(1)}\otimes\begin{pmatrix}e_j\\ f_j\end{pmatrix}, & 2\le j\le \frac{N+1}{2},\\ -\frac{1}{\sqrt{2N}}\boldsymbol{\phi}^{(2(N+2-j)-1)}\otimes\begin{pmatrix}e_j\\ f_j\end{pmatrix}+\frac{1}{\sqrt{N}}\boldsymbol{\phi}^{(1)}\otimes\begin{pmatrix}e_j\\ f_j\end{pmatrix}, & \frac{N+3}{2}\le j\le N.\end{cases} \tag{A.9}$$

By (2.22), we obtain

$$\begin{cases}\boldsymbol{w}_{20}=[I_N\otimes(2i\omega_j I_2)-\boldsymbol{M}(\mu_{j,\pm}^H(G_{la}))]^{-1}\boldsymbol{H}_{20},\\ \boldsymbol{w}_{11}=-[\boldsymbol{M}(\mu_{j,\pm}^H(G_{la}))]^{-1}\boldsymbol{H}_{11}.\end{cases} \tag{A.10}$$

From (A.8) and (A.9), together with Lemma 2.1, we obtain that, when N is odd,

$$\boldsymbol{w}_{20}=\begin{cases}\frac{1}{\sqrt{2N}}\boldsymbol{\phi}^{(2j-1)}\otimes\left\{\left[2i\omega_j\boldsymbol{I}_2-\boldsymbol{M}_{(2j-1)}(\mu_{j,\pm}^H(G_{la}))\right]^{-1}\begin{pmatrix}c_j\\ d_j\end{pmatrix}\right\}\\ \quad+\frac{1}{\sqrt{N}}\boldsymbol{\phi}^{(1)}\otimes\left\{\left[2i\omega_j\boldsymbol{I}_2-\boldsymbol{M}_1(\mu_{j,\pm}^H(G_{la}))\right]^{-1}\begin{pmatrix}c_j\\ d_j\end{pmatrix}\right\}, & 2\le j\le\frac{N+1}{2},\\ -\frac{1}{\sqrt{2N}}\boldsymbol{\phi}^{(2(N+2-j)-1)}\otimes\left\{\left[2i\omega_j\boldsymbol{I}_2-\boldsymbol{M}_{(2(N+2-j)-1)}(\mu_{j,\pm}^H(G_{la}))\right]^{-1}\begin{pmatrix}c_j\\ d_j\end{pmatrix}\right\}\\ \quad+\frac{1}{\sqrt{N}}\boldsymbol{\phi}^{(1)}\otimes\left\{\left[2i\omega_j\boldsymbol{I}_2-\boldsymbol{M}_1(\mu_{j,\pm}^H(G_{la}))\right]^{-1}\begin{pmatrix}c_j\\ d_j\end{pmatrix}\right\}, & \frac{N+3}{2}\le j\le N,\end{cases} \tag{A.11}$$

and

$$\boldsymbol{w}_{11}=\begin{cases}\frac{1}{\sqrt{2N}}\boldsymbol{\phi}^{(2j-1)}\otimes\left\{\left[-\boldsymbol{M}_{(2j-1)}(\mu_{j,\pm}^H(G_{la}))\right]^{-1}\begin{pmatrix}e_j\\ f_j\end{pmatrix}\right\}\\ \quad+\frac{1}{\sqrt{N}}\boldsymbol{\phi}^{(1)}\otimes\left\{\left[-\boldsymbol{M}_1(\mu_{j,\pm}^H(G_{la}))\right]^{-1}\begin{pmatrix}e_j\\ f_j\end{pmatrix}\right\}, & 2\le j\le\frac{N+1}{2},\\ -\frac{1}{\sqrt{2N}}\boldsymbol{\phi}^{(2(N+2-j)-1)}\otimes\left\{\left[-\boldsymbol{M}_{(2(N+2-j)-1)}(\mu_{j,\pm}^H(G_{la}))\right]^{-1}\begin{pmatrix}e_j\\ f_j\end{pmatrix}\right\}\\ \quad+\frac{1}{\sqrt{N}}\boldsymbol{\phi}^{(1)}\otimes\left\{\left[-\boldsymbol{M}_1(\mu_{j,\pm}^H(G_{la}))\right]^{-1}\begin{pmatrix}e_j\\ f_j\end{pmatrix}\right\}, & \frac{N+3}{2}\le j\le N.\end{cases} \tag{A.12}$$

It is straightforward to compute that

$$\Big[2i\omega_j \boldsymbol{I}_2 - \boldsymbol{M}_{(2j-1)}(\mu^H_{j,\pm}(G_{la}))\Big]^{-1} = (\alpha_1 + i\alpha_2)^{-1}\begin{pmatrix} 2i\omega_j + P_{41} & -\theta \\ C(\mu^H_{j,\pm}(G_{la})) & 2i\omega_j + P_{51} \end{pmatrix},$$

$$\Big[2i\omega_j \boldsymbol{I}_2 - \boldsymbol{M}_{(2(N+2-j)-1)}(\mu^H_{j,\pm}(G_{la}))\Big]^{-1} = (\alpha_3 + i\alpha_4)^{-1}\begin{pmatrix} 2i\omega_j + P_{42} & -\theta \\ C(\mu^H_{j,\pm}(G_{la})) & 2i\omega_j + P_{52} \end{pmatrix},$$

$$\Big[2i\omega_j \boldsymbol{I}_2 - \boldsymbol{M}_{1}(\mu^H_{j,\pm}(G_{la}))\Big]^{-1} = (\alpha_5 + i\alpha_6)^{-1}\begin{pmatrix} 2i\omega_j & -\theta \\ C(\mu^H_{j,\pm}(G_{la})) & 2i\omega_j + P_{6} \end{pmatrix},$$

$$\Big[- \boldsymbol{M}_{(2j-1)}(\mu^H_{j,\pm}(G_{la}))\Big]^{-1} = \alpha_7^{-1}\begin{pmatrix} P_{41} & -\theta \\ C(\mu^H_{j,\pm}(G_{la})) & P_{51} \end{pmatrix},$$

$$\Big[- \boldsymbol{M}_{(2(N+2-j)-1)}(\mu^H_{j,\pm}(G_{la}))\Big]^{-1} = \alpha_8^{-1}\begin{pmatrix} P_{42} & -\theta \\ C(\mu^H_{j,\pm}(G_{la})) & P_{52} \end{pmatrix},$$

$$\Big[- \boldsymbol{M}_{1}(\mu^H_{j,\pm}(G_{la}))\Big]^{-1} = \frac{1}{\theta C(\mu^H_{j,\pm}(G_{la}))}\begin{pmatrix} 0 & -\theta \\ C(\mu^H_{j,\pm}(G_{la})) & P_{6} \end{pmatrix},$$

with

$$\begin{aligned}
\alpha_1 &= 4d_u d_v\Big[\cos\frac{2(j-1)\pi}{N} - \cos\frac{(j-1)\pi}{N}\Big]\Big[\cos\frac{2(j-1)\pi}{N} - 1\Big] \\
&\quad + 4d_v^2\Big[\cos\frac{(j-1)\pi}{N} - 1\Big]\Big[\cos\frac{(j-1)\pi}{N} - \cos\frac{2(j-1)\pi}{N}\Big] - 3\omega_j^2, \\
\alpha_2 &= -4\omega_j(d_u + d_v)\Big[\cos\frac{2(j-1)\pi}{N} - \cos\frac{(j-1)\pi}{N}\Big], \\
\alpha_3 &= 4d_u d_v\Big[\cos\frac{2(N+1-j)\pi}{N} - \cos\frac{(j-1)\pi}{N}\Big]\Big[\cos\frac{2(N+1-j)\pi}{N} - 1\Big] \\
&\quad + 4d_v^2\Big[\cos\frac{(j-1)\pi}{N} - 1\Big]\Big[\cos\frac{(j-1)\pi}{N} - \cos\frac{2(N+1-j)\pi}{N}\Big] - 3\omega_j^2, \\
\alpha_4 &= -4\omega_j(d_u + d_v)\Big[\cos\frac{2(N+1-j)\pi}{N} - \cos\frac{(j-1)\pi}{N}\Big], \\
\alpha_5 &= 4d_v^2\Big[\cos\frac{(j-1)\pi}{N} - 1\Big]^2 - 3\omega_j^2, \\
\alpha_6 &= 4\omega_j(d_u + d_v)\Big[\cos\frac{(j-1)\pi}{N} - 1\Big], \\
\alpha_7 &= 4d_u d_v\Big[\cos\frac{2(j-1)\pi}{N} - \cos\frac{(j-1)\pi}{N}\Big]\Big[\cos\frac{2(j-1)\pi}{N} - 1\Big] \\
&\quad + 4d_v^2\Big[\cos\frac{(j-1)\pi}{N} - 1\Big]\Big[\cos\frac{(j-1)\pi}{N} - \cos\frac{2(j-1)\pi}{N}\Big] + \omega_j^2, \\
\alpha_8 &= 4d_u d_v\Big[\cos\frac{2(N+1-j)\pi}{N} - \cos\frac{(j-1)\pi}{N}\Big]\Big[\cos\frac{2(N+1-j)\pi}{N} - 1\Big] \\
&\quad + 4d_v^2\Big[\cos\frac{(j-1)\pi}{N} - 1\Big]\Big[\cos\frac{(j-1)\pi}{N} - \cos\frac{2(N+1-j)\pi}{N}\Big] + \omega_j^2,
\end{aligned}$$

and

$$
\begin{aligned}
P_{41} &= -2d_v\Big[\cos\frac{2(j-1)\pi}{N}-1\Big],\\
P_{42} &= -2d_v\Big[\cos\frac{2(N+1-j)\pi}{N}-1\Big],\\
P_{51} &= 2d_u\Big[\cos\frac{2(j-1)\pi}{N}-\cos\frac{(j-1)\pi}{N}\Big]-2d_v\Big[\cos\frac{(j-1)\pi}{N}-1\Big],\\
P_{52} &= -2d_u\Big[\cos\frac{2(N+1-j)\pi}{N}-\cos\frac{(j-1)\pi}{N}\Big]-2d_v\Big[\cos\frac{(j-1)\pi}{N}-1\Big],\\
P_6 &= 2(d_u+d_v)\Big[\cos\frac{(j-1)\pi}{N}-1\Big].
\end{aligned}
$$

For simplicity of notations, we denote

$$
\boldsymbol{w}_{20}=\boldsymbol{\phi}^{(j^*)}\otimes\begin{pmatrix}\xi^{(j^*)}\\ \eta^{(j^*)}\end{pmatrix}+\boldsymbol{\phi}^{(1)}\otimes\begin{pmatrix}\tau\\ \chi\end{pmatrix} \tag{A.13}
$$

with

$$
\begin{aligned}
\xi^{(j^*)}&=\xi_R^{(j^*)}+i\xi_{Im}^{(j^*)}, &\quad \eta^{(j^*)}&=\eta_R^{(j^*)}+i\eta_{Im}^{(j^*)},\\
\tau&=\tau_R+i\tau_{Im}, & \chi&=\chi_R+i\chi_{Im},
\end{aligned}
$$

and

$$
\boldsymbol{w}_{11}=\boldsymbol{\phi}^{(j^*)}\otimes\begin{pmatrix}\widetilde{\xi}^{(j^*)}\\ \widetilde{\eta}^{(j^*)}\end{pmatrix}+\boldsymbol{\phi}^{(1)}\otimes\begin{pmatrix}\widetilde{\tau}\\ \widetilde{\chi}\end{pmatrix} \tag{A.14}
$$

where

$$
\xi_R^{(j^*)}=\begin{cases}
\frac{\alpha_1}{\sqrt{2N}(\alpha_1^2+\alpha_2^2)}\big[P_{41}(f_{uu}+P_1f_{uv})-2P_2\omega_jf_{uv}-\theta(g_{uu}+P_1g_{uv})\big]\\
\quad+\frac{\alpha_2}{\sqrt{2N}(\alpha_1^2+\alpha_2^2)}\big[P_{41}P_2f_{uv}+2\omega_j(f_{uu}+P_1f_{uv})-\theta P_2g_{uv}\big],\\
\qquad j^*=2j-1,\ \text{for } 2\le j\le\frac{N+1}{2},\ \text{if } N \text{ is odd},\\
\frac{\alpha_3}{\sqrt{2N}(\alpha_3^2+\alpha_4^2)}\big[P_{42}(f_{uu}+P_1f_{uv})-2P_2\omega_jf_{uv}-\theta(g_{uu}+P_1g_{uv})\big]\\
\quad+\frac{\alpha_4}{\sqrt{2N}(\alpha_3^2+\alpha_4^2)}\big[P_{42}P_2f_{uv}+2\omega_j(f_{uu}+P_1f_{uv})-\theta P_2g_{uv}\big],\\
\qquad j^*=2(N+2-j)-1,\ \text{for } \frac{N+3}{2}\le j\le N,\ \text{if } N \text{ is odd},
\end{cases}
$$

$$
\xi_{Im}^{(j^*)}=\begin{cases}
\frac{\alpha_1}{\sqrt{2N}(\alpha_1^2+\alpha_2^2)}\big[P_{41}P_2f_{uv}+2\omega_j(f_{uu}+P_1f_{uv})-\theta P_2g_{uv}\big]\\
\quad-\frac{\alpha_2}{\sqrt{2N}(\alpha_1^2+\alpha_2^2)}\big[P_{41}(f_{uu}+P_1f_{uv})-2P_2\omega_jf_{uv}-\theta(g_{uu}+P_1g_{uv})\big],\\
\qquad j^*=2j-1,\ \text{for } 2\le j\le\frac{N+1}{2},\ \text{if } N \text{ is odd},\\
\frac{\alpha_3}{\sqrt{2N}(\alpha_3^2+\alpha_4^2)}\big[P_{42}P_2f_{uv}+2\omega_j(f_{uu}+P_1f_{uv})-\theta P_2g_{uv}\big]\\
\quad-\frac{\alpha_4}{\sqrt{2N}(\alpha_3^2+\alpha_4^2)}\big[P_{42}(f_{uu}+P_1f_{uv})-2P_2\omega_jf_{uv}-\theta(g_{uu}+P_1g_{uv})\big],\\
\qquad j^*=2(N+2-j)-1,\ \text{for } \frac{N+3}{2}\le j\le N,\ \text{if } N \text{ is odd},
\end{cases}
\tag{A.15a}
$$

and

$$\eta_R^{(j^*)} = \begin{cases} \frac{\alpha_1}{\sqrt{2N}(\alpha_1^2+\alpha_2^2)}\big[C(\mu_{j,\pm}^H(G_{la}))(f_{uu}+P_1 f_{uv}) + P_{51}(g_{uu}+P_1 g_{uv}) - 2P_2\omega_j g_{uv}\big] \\ \quad + \frac{\alpha_2}{\sqrt{2N}(\alpha_1^2+\alpha_2^2)}\big[C(\mu_{j,\pm}^H(G_{la}))P_2 f_{uv} + 2\omega_j(g_{uu}+P_1 g_{uv}) + P_{51}P_2 g_{uv}\big], \\ \qquad j^* = 2j-1, \text{ for } 2 \le j \le \frac{N+1}{2}, \text{ if } N \text{ is odd}, \\ \frac{\alpha_3}{\sqrt{2N}(\alpha_3^2+\alpha_4^2)}\big[C(\mu_{j,\pm}^H(G_{la}))(f_{uu}+P_1 f_{uv}) + P_{52}(g_{uu}+P_1 g_{uv}) - 2P_2\omega_j g_{uv}\big] \\ \quad + \frac{\alpha_4}{\sqrt{2N}(\alpha_3^2+\alpha_4^2)}\big[C(\mu_{j,\pm}^H(G_{la}))P_2 f_{uv} + 2\omega_j(g_{uu}+P_1 g_{uv}) + P_{52}P_2 g_{uv}\big], \\ \qquad j^* = 2(N+2-j)-1, \text{ for } \frac{N+3}{2} \le j \le N, \text{ if } N \text{ is odd}, \end{cases}$$

$$\eta_{Im}^{(j^*)} = \begin{cases} \frac{\alpha_1}{\sqrt{2N}(\alpha_1^2+\alpha_2^2)}\big[C(\mu_{j,\pm}^H(G_{la}))P_2 f_{uv} + 2\omega_j(g_{uu}+P_1 g_{uv}) + P_{51}P_2 g_{uv}\big] \\ \quad - \frac{\alpha_2}{\sqrt{2N}(\alpha_1^2+\alpha_2^2)}\big[C(\mu_{j,\pm}^H(G_{la}))(f_{uu}+P_1 f_{uv}) + P_{51}(g_{uu}+P_1 g_{uv}) - 2P_2\omega_j g_{uv}\big], \\ \qquad j^* = 2j-1, \text{ for } 2 \le j \le \frac{N+1}{2}, \text{ if } N \text{ is odd}, \\ \frac{\alpha_3}{\sqrt{2N}(\alpha_3^2+\alpha_4^2)}\big[C(\mu_{j,\pm}^H(G_{la}))P_2 f_{uv} + 2\omega_j(g_{uu}+P_1 g_{uv}) + P_{52}P_2 g_{uv}\big] \\ \quad - \frac{\alpha_4}{\sqrt{2N}(\alpha_3^2+\alpha_4^2)}\big[C(\mu_{j,\pm}^H(G_{la}))(f_{uu}+P_1 f_{uv}) + P_{52}(g_{uu}+P_1 g_{uv}) - 2P_2\omega_j g_{uv}\big], \\ \qquad j^* = 2(N+2-j)-1, \text{ for } \frac{N+3}{2} \le j \le N, \text{ if } N \text{ is odd}, \end{cases} \tag{A.15b}$$

and

$$\begin{aligned} \tau_R &= \frac{\alpha_5}{\sqrt{N}(\alpha_5^2+\alpha_6^2)}\big[-2P_2\omega_j f_{uv} - \theta(g_{uu}+P_1 g_{uv})\big] \\ &\quad + \frac{\alpha_6}{\sqrt{N}(\alpha_5^2+\alpha_6^2)}\big[2\omega_j(f_{uu}+P_1 f_{uv}) - \theta P_2 g_{uv}\big], \\ \tau_{Im} &= \frac{\alpha_5}{\sqrt{N}(\alpha_5^2+\alpha_6^2)}\big[2\omega_j(f_{uu}+P_1 f_{uv}) - \theta P_2 g_{uv}\big] \\ &\quad - \frac{\alpha_6}{\sqrt{N}(\alpha_5^2+\alpha_6^2)}\big[-2P_2\omega_j f_{uv} - \theta(g_{uu}+P_1 g_{uv})\big], \\ \chi_R &= \frac{\alpha_5}{\sqrt{N}(\alpha_5^2+\alpha_6^2)}\big[C(\mu_{j,\pm}^H(G_{la}))(f_{uu}+P_1 f_{uv}) + P_6(g_{uu}+P_1 g_{uv}) - 2P_2\omega_j g_{uv}\big] \\ &\quad + \frac{\alpha_6}{\sqrt{N}(\alpha_5^2+\alpha_6^2)}\big[C(\mu_{j,\pm}^H(G_{la}))P_2 f_{uv} + 2\omega_j(g_{uu}+P_1 g_{uv}) + P_6 P_2 g_{uv}\big], \\ \chi_{Im} &= \frac{\alpha_5}{\sqrt{N}(\alpha_5^2+\alpha_6^2)}\big[C(\mu_{j,\pm}^H(G_{la}))P_2 f_{uv} + 2\omega_j(g_{uu}+P_1 g_{uv}) + P_6 P_2 g_{uv}\big] \\ &\quad - \frac{\alpha_6}{\sqrt{N}(\alpha_5^2+\alpha_6^2)}\big[C(\mu_{j,\pm}^H(G_{la}))(f_{uu}+P_1 f_{uv}) + P_6(g_{uu}+P_1 g_{uv}) - 2P_2\omega_j g_{uv}\big], \end{aligned} \tag{A.15c}$$

and

$$\widetilde{\xi}^{(j^*)} = \begin{cases} \frac{1}{\sqrt{2N}\alpha_7}\big[P_{41}(f_{uu}+P_1 f_{uv}) - \theta(g_{uu}+P_1 g_{uv})\big], \\ \qquad j^* = 2j-1, \text{ for } 2 \le j \le \frac{N+1}{2}, \text{ if } N \text{ is odd}, \\ \frac{1}{\sqrt{2N}\alpha_8}\big[P_{42}(f_{uu}+P_1 f_{uv}) - \theta(g_{uu}+P_1 g_{uv})\big], \\ \qquad j^* = 2(N+2-j)-1, \text{ for } \frac{N+3}{2} \le j \le N, \text{ if } N \text{ is odd}, \end{cases}$$
$$\widetilde{\eta}^{(j^*)} = \begin{cases} \frac{1}{\sqrt{2N}\alpha_7}\big[C(\mu^H_{j,\pm}(G_{la}))(f_{uu}+P_1 f_{uv}) + P_{51}(g_{uu}+P_1 g_{uv})\big], \\ \qquad j^* = 2j-1, \text{ for } 2 \le j \le \frac{N+1}{2}, \text{ if } N \text{ is odd}, \\ \frac{1}{\sqrt{2N}\alpha_8}\big[C(\mu^H_{j,\pm}(G_{la}))(f_{uu}+P_1 f_{uv}) + P_{52}(g_{uu}+P_1 g_{uv})\big], \\ \qquad j^* = 2(N+2-j)-1, \text{ for } \frac{N+3}{2} \le j \le N, \text{ if } N \text{ is odd}, \end{cases} \tag{A.15d}$$

and

$$\widetilde{\tau} = -\frac{1}{\sqrt{N}C(\mu^H_{j,\pm}(G_{la}))}(g_{uu}+P_1 g_{uv}),$$
$$\widetilde{\chi} = \frac{1}{\sqrt{N}\theta C(\mu^H_{j,\pm}(G_{la}))}\Big[C(\mu^H_{j,\pm}(G_{la}))(f_{uu}+P_1 f_{uv}) + P_6(g_{uu}+P_1 g_{uv})\Big]. \tag{A.15e}$$

Therefore, we have

$$\begin{aligned} Q_{\boldsymbol{w}_{20}\overline{\boldsymbol{q}}} &= \operatorname{col}\begin{pmatrix} [f_{uu}\xi^{(j^*)} + f_{uv}(\eta^{(j^*)} + \overline{b_j}\xi^{(j^*)})]\phi_l^{(j^*)}\phi_l^{(j)} \\ [g_{uu}\xi^{(j^*)} + g_{uv}(\eta^{(j^*)} + \overline{b_j}\xi^{(j^*)})]\phi_l^{(j^*)}\phi_l^{(j)} \end{pmatrix}_{l=1}^{l=N} \\ &\quad + \operatorname{col}\begin{pmatrix} [f_{uu}\tau + f_{uv}(\chi + \overline{b_j}\tau)]\phi_l^{(1)}\phi_l^{(j)} \\ [g_{uu}\tau + g_{uv}(\chi + \overline{b_j}\tau)]\phi_l^{(1)}\phi_l^{(j)} \end{pmatrix}_{l=1}^{l=N}, \end{aligned} \tag{A.16}$$

$$\begin{aligned} Q_{\boldsymbol{w}_{11}\boldsymbol{q}} &= \operatorname{col}\begin{pmatrix} [f_{uu}\widetilde{\xi}^{(j^*)} + f_{uv}(\widetilde{\eta}^{(j^*)} + b_j\widetilde{\xi}^{(j^*)})]\phi_l^{(j^*)}\phi_l^{(j)} \\ [g_{uu}\widetilde{\xi}^{(j^*)} + g_{uv}(\widetilde{\eta}^{(j^*)} + b_j\widetilde{\xi}^{(j^*)})]\phi_l^{(j^*)}\phi_l^{(j)} \end{pmatrix}_{l=1}^{l=N} \\ &\quad + \operatorname{col}\begin{pmatrix} [f_{uu}\widetilde{\tau} + f_{uv}(\widetilde{\chi} + b_j\widetilde{\tau})]\phi_l^{(1)}\phi_l^{(j)} \\ [g_{uu}\widetilde{\tau} + g_{uv}(\widetilde{\chi} + b_j\widetilde{\tau})]\phi_l^{(1)}\phi_l^{(j)} \end{pmatrix}_{l=1}^{l=N}. \end{aligned} \tag{A.17}$$

And then, we have

$$\begin{aligned} \langle \boldsymbol{q}^*, Q_{\boldsymbol{w}_{20}\overline{\boldsymbol{q}}}\rangle &= \Big\{\overline{a_j^*}[f_{uu}\xi^{(j^*)} + f_{uv}(\eta^{(j^*)} + \overline{b_j}\xi^{(j^*)})] \\ &\quad + \overline{b_j^*}[g_{uu}\xi^{(j^*)} + g_{uv}(\eta^{(j^*)} + \overline{b_j}\xi^{(j^*)})]\Big\}\sum_{l=1}^{N}\phi_l^{(j^*)}\big(\phi_l^{(j)}\big)^2 \\ &\quad + \Big\{\overline{a_j^*}[f_{uu}\tau + f_{uv}(\chi + \overline{b_j}\tau)] + \overline{b_j^*}[g_{uu}\tau + g_{uv}(\chi + \overline{b_j}\tau)]\Big\}\sum_{l=1}^{N}\phi_l^{(1)}\big(\phi_l^{(j)}\big)^2. \end{aligned} \tag{A.18}$$

and

$$\begin{aligned}\langle \boldsymbol{q}^*, Q_{\boldsymbol{w}_{11}\boldsymbol{q}}\rangle = \Big\{&\overline{a_j^*}[f_{uu}\widetilde{\xi}^{(j^*)} + f_{uv}(\widetilde{\eta}^{(j^*)} + b_j\widetilde{\xi}^{(j^*)})] \\ &+ \overline{b_j^*}[g_{uu}\widetilde{\xi}^{(j^*)} + g_{uv}(\widetilde{\eta}^{(j^*)} + b_j\widetilde{\xi}^{(j^*)})]\Big\}\sum_{l=1}^{N}\phi_l^{(j^*)}\big(\phi_l^{(j)}\big)^2 \\ &+ \Big\{\overline{a_j^*}[f_{uu}\widetilde{\tau} + f_{uv}(\widetilde{\chi} + b_j\widetilde{\tau})] + \overline{b_j^*}[g_{uu}\widetilde{\tau} + g_{uv}(\widetilde{\chi} + b_j\widetilde{\tau})]\Big\}\sum_{l=1}^{N}\phi_l^{(1)}\big(\phi_l^{(j)}\big)^2.\end{aligned} \tag{A.19}$$

Therefore,

$$\begin{aligned}&\mathrm{Re}\big(\langle \boldsymbol{q}^*, Q_{\boldsymbol{w}_{20}\overline{\boldsymbol{q}}}\rangle\big) \\ &= \Bigg\{\frac{1}{2}\Big[f_{uu}\xi_R^{(j^*)} + f_{uv}\Big(\eta_R^{(j^*)} - \frac{2d_v}{\theta}\big(\cos\frac{(j-1)\pi}{N} - 1\big)\xi_R^{(j^*)} - \frac{\omega_j}{\theta}\xi_{Im}^{(j^*)}\Big)\Big] \\ &- \frac{d_v}{\omega_j}\big(\cos\frac{(j-1)\pi}{N} - 1\big)\Big[f_{uu}\xi_{Im}^{(j^*)} + f_{uv}\Big(\eta_{Im}^{(j^*)} - \frac{2d_v}{\theta}\big(\cos\frac{(j-1)\pi}{N} - 1\big)\xi_{Im}^{(j^*)} + \frac{\omega_j}{\theta}\xi_R^{(j^*)}\Big)\Big] \\ &- \frac{\theta}{2\omega_j}\Big[g_{uu}\xi_{Im}^{(j^*)} + g_{uv}\Big(\eta_{Im}^{(j^*)} - \frac{2d_v}{\theta}\big(\cos\frac{(j-1)\pi}{N} - 1\big)\xi_{Im}^{(j^*)} + \frac{\omega_j}{\theta}\xi_R^{(j^*)}\Big)\Big]\Bigg\}\sum_{l=1}^{N}\phi_l^{(j^*)}\big(\phi_l^{(j)}\big)^2 \\ &+ \Bigg\{\frac{1}{2}\Big[f_{uu}\tau_R + f_{uv}\Big(\chi_R - \frac{2d_v}{\theta}\big(\cos\frac{(j-1)\pi}{N} - 1\big)\tau_R - \frac{\omega_j}{\theta}\tau_{Im}\Big)\Big] \\ &- \frac{d_v}{\omega_j}\big(\cos\frac{(j-1)\pi}{N} - 1\big)\Big[f_{uu}\tau_{Im} + f_{uv}\Big(\chi_{Im} - \frac{2d_v}{\theta}\big(\cos\frac{(j-1)\pi}{N} - 1\big)\tau_{Im} + \frac{\omega_j}{\theta}\tau_R\Big)\Big] \\ &- \frac{\theta}{2\omega_j}\Big[g_{uu}\tau_{Im} + g_{uv}\Big(\chi_{Im} - \frac{2d_v}{\theta}\big(\cos\frac{(j-1)\pi}{N} - 1\big)\tau_{Im} + \frac{\omega_j}{\theta}\tau_R\Big)\Big]\Bigg\}\sum_{l=1}^{N}\phi_l^{(1)}\big(\phi_l^{(j)}\big)^2, \\ &\mathrm{Re}\big(\langle \boldsymbol{q}^*, Q_{\boldsymbol{w}_{11}\boldsymbol{q}}\rangle\big) \\ &= \frac{1}{2}\Big(f_{uu}\widetilde{\xi}^{(j^*)} + f_{uv}\widetilde{\eta}^{(j^*)} + g_{uv}\widetilde{\xi}^{(j^*)}\Big)\sum_{l=1}^{N}\phi_l^{(j^*)}\big(\phi_l^{(j)}\big)^2 \\ &+ \frac{1}{2}\Big(f_{uu}\widetilde{\tau} + f_{uv}\widetilde{\chi} + g_{uv}\widetilde{\tau}\Big)\sum_{l=1}^{N}\phi_l^{(1)}\big(\phi_l^{(j)}\big)^2.\end{aligned} \tag{A.20}$$

At the same time, we have

$$\langle \boldsymbol{q}^*, C_{\boldsymbol{q}\boldsymbol{q}\bar{\boldsymbol{q}}}\rangle = \big(\overline{a_j^*}g_j + \overline{b_j^*}h_j\big)\sum_{l=1}^{N}\big(\phi_l^{(j)}\big)^4, \tag{A.21}$$

and, hence

$$\operatorname{Re}\big(\langle \boldsymbol{q}^*, C_{\boldsymbol{q}\boldsymbol{q}\bar{\boldsymbol{q}}}\rangle\big) = \frac{1}{2}\big(f_{uuu} - \frac{4d_v}{\theta}\big(\cos\frac{(j-1)\pi}{N} - 1\big) f_{uuv} + g_{uuv}\big) \sum_{l=1}^{N} \big(\phi_l^{(j)}\big)^4. \tag{A.22}$$

Indeed, when N is odd, for $j = 2, 3, \dots, N$, we have

$$\sum_{l=1}^{N} \big(\phi_l^{(j)}\big)^4 = \frac{3}{2N}, \quad \sum_{l=1}^{N} \phi_l^{(1)} \big(\phi_l^{(j)}\big)^2 = \frac{1}{\sqrt{N}},$$
$$\sum_{l=1}^{N} \phi_l^{(j^*)} \big(\phi_l^{(j)}\big)^2 = \begin{cases} \frac{1}{\sqrt{2N}}, & j^* = 2j-1, \text{ for } 2 \le j \le \frac{N+1}{2}, \\ -\frac{1}{\sqrt{2N}}, & j^* = 2(N+2-j)-1, \text{ for } \frac{N+3}{2} \le j \le N. \end{cases}$$

So, and so far, by (2.27), when N is odd, for $2 \le j \le \frac{N+1}{2}$, we have

$$\begin{aligned}
&\operatorname{Re}\big(c_1(\mu_{j,\pm}^H(G_{la}))\big) \\
&= \operatorname{Re}\big(\langle \boldsymbol{q}^*, Q_{\boldsymbol{w}_{11}\boldsymbol{q}}\rangle\big) + \frac{1}{2}\operatorname{Re}\big(\langle \boldsymbol{q}^*, Q_{\boldsymbol{w}_{20}\bar{\boldsymbol{q}}}\rangle\big) + \frac{1}{2}\operatorname{Re}\big(\langle \boldsymbol{q}^*, C_{\boldsymbol{q}\boldsymbol{q}\bar{\boldsymbol{q}}}\rangle\big) \\
&= \frac{1}{2\sqrt{2N}}\Big(f_{uu}\widetilde{\xi}^{(j^*)} + f_{uv}\widetilde{\eta}^{(j^*)} + g_{uv}\widetilde{\xi}^{(j^*)}\Big) + \frac{1}{2\sqrt{N}}\Big(f_{uu}\widetilde{\tau} + f_{uv}\widetilde{\chi} + g_{uv}\widetilde{\tau}\Big) \\
&+ \frac{1}{4\sqrt{2N}}\Bigg\{\Big[f_{uu}\xi_R^{(j^*)} + f_{uv}\Big(\eta_R^{(j^*)} - \frac{2d_v}{\theta}\big(\cos\frac{(j-1)\pi}{N} - 1\big)\xi_R^{(j^*)} - \frac{\omega_j}{\theta}\xi_{Im}^{(j^*)}\Big)\Big] \\
&- \frac{2d_v}{\omega_j}\big(\cos\frac{(j-1)\pi}{N} - 1\big)\Big[f_{uu}\xi_{Im}^{(j^*)} + f_{uv}\Big(\eta_{Im}^{(j^*)} - \frac{2d_v}{\theta}\big(\cos\frac{(j-1)\pi}{N} - 1\big)\xi_{Im}^{(j^*)} + \frac{\omega_j}{\theta}\xi_R^{(j^*)}\Big)\Big] \\
&- \frac{\theta}{\omega_j}\Big[g_{uu}\xi_{Im}^{(j^*)} + g_{uv}\Big(\eta_{Im}^{(j^*)} - \frac{2d_v}{\theta}\big(\cos\frac{(j-1)\pi}{N} - 1\big)\xi_{Im}^{(j^*)} + \frac{\omega_j}{\theta}\xi_R^{(j^*)}\Big)\Big]\Bigg\} \\
&+ \frac{1}{4\sqrt{N}}\Bigg\{\Big[f_{uu}\tau_R + f_{uv}\Big(\chi_R - \frac{2d_v}{\theta}\big(\cos\frac{(j-1)\pi}{N} - 1\big)\tau_R - \frac{\omega_j}{\theta}\tau_{Im}\Big)\Big] \\
&- \frac{2d_v}{\omega_j}\big(\cos\frac{(j-1)\pi}{N} - 1\big)\Big[f_{uu}\tau_{Im} + f_{uv}\Big(\chi_{Im} - \frac{2d_v}{\theta}\big(\cos\frac{(j-1)\pi}{N} - 1\big)\tau_{Im} + \frac{\omega_j}{\theta}\tau_R\Big)\Big] \\
&- \frac{\theta}{\omega_j}\Big[g_{uu}\tau_{Im} + g_{uv}\Big(\chi_{Im} - \frac{2d_v}{\theta}\big(\cos\frac{(j-1)\pi}{N} - 1\big)\tau_{Im} + \frac{\omega_j}{\theta}\tau_R\Big)\Big]\Bigg\} \\
&+ \frac{3}{8N}\Big[f_{uuu} - \frac{4d_v}{\theta}\big(\cos\frac{(j-1)\pi}{N} - 1\big) f_{uuv} + g_{uuv}\Big].
\end{aligned} \tag{A.23}$$

For $\frac{N+3}{2} \le j \le N$, we have

$$
\begin{aligned}
&\mathrm{Re}\big(c_1(\mu^H_{j,\pm}(G_{la}))\big)\\
&=\mathrm{Re}\big(\langle \boldsymbol{q}^*, Q_{\boldsymbol{w}_{11}\boldsymbol{q}}\rangle\big)+\frac{1}{2}\mathrm{Re}\big(\langle \boldsymbol{q}^*, Q_{\boldsymbol{w}_{20}\bar{\boldsymbol{q}}}\rangle\big)+\frac{1}{2}\mathrm{Re}\big(\langle \boldsymbol{q}^*, C_{\boldsymbol{q}\boldsymbol{q}\bar{\boldsymbol{q}}}\rangle\big)\\
&=-\frac{1}{2\sqrt{2N}}\Big(f_{uu}\widetilde{\xi}^{(j^*)}+f_{uv}\widetilde{\eta}^{(j^*)}+g_{uv}\widetilde{\xi}^{(j^*)}\Big)+\frac{1}{2\sqrt{N}}\Big(f_{uu}\widetilde{\tau}+f_{uv}\widetilde{\chi}+g_{uv}\widetilde{\tau}\Big)\\
&-\frac{1}{4\sqrt{2N}}\Bigg\{\Big[f_{uu}\xi_R^{(j^*)}+f_{uv}\Big(\eta_R^{(j^*)}-\frac{2d_v}{\theta}\big(\cos\frac{(j-1)\pi}{N}-1\big)\xi_R^{(j^*)}-\frac{\omega_j}{\theta}\xi_{Im}^{(j^*)}\Big)\Big]\\
&-\frac{2d_v}{\omega_j}\big(\cos\frac{(j-1)\pi}{N}-1\big)\Big[f_{uu}\xi_{Im}^{(j^*)}+f_{uv}\Big(\eta_{Im}^{(j^*)}-\frac{2d_v}{\theta}\big(\cos\frac{(j-1)\pi}{N}-1\big)\xi_{Im}^{(j^*)}+\frac{\omega_j}{\theta}\xi_R^{(j^*)}\Big)\Big]\\
&-\frac{\theta}{\omega_j}\Big[g_{uu}\xi_{Im}^{(j^*)}+g_{uv}\Big(\eta_{Im}^{(j^*)}-\frac{2d_v}{\theta}\big(\cos\frac{(j-1)\pi}{N}-1\big)\xi_{Im}^{(j^*)}+\frac{\omega_j}{\theta}\xi_R^{(j^*)}\Big)\Big]\Bigg\}\\
&+\frac{1}{4\sqrt{N}}\Bigg\{\Big[f_{uu}\tau_R+f_{uv}\Big(\chi_R-\frac{2d_v}{\theta}\big(\cos\frac{(j-1)\pi}{N}-1\big)\tau_R-\frac{\omega_j}{\theta}\tau_{Im}\Big)\Big]\\
&-\frac{2d_v}{\omega_j}\big(\cos\frac{(j-1)\pi}{N}-1\big)\Big[f_{uu}\tau_{Im}+f_{uv}\Big(\chi_{Im}-\frac{2d_v}{\theta}\big(\cos\frac{(j-1)\pi}{N}-1\big)\tau_{Im}+\frac{\omega_j}{\theta}\tau_R\Big)\Big]\\
&-\frac{\theta}{\omega_j}\Big[g_{uu}\tau_{Im}+g_{uv}\Big(\chi_{Im}-\frac{2d_v}{\theta}\big(\cos\frac{(j-1)\pi}{N}-1\big)\tau_{Im}+\frac{\omega_j}{\theta}\tau_R\Big)\Big]\Bigg\}\\
&+\frac{3}{8N}\Big[f_{uuu}-\frac{4d_v}{\theta}\big(\cos\frac{(j-1)\pi}{N}-1\big)f_{uuv}+g_{uuv}\Big].
\end{aligned}
\tag{A.24}
$$

For the other case where N is even, we can compute $\mathrm{Re}(c_1(\mu^H_{j,\pm}(G_{la})))$ in a similar way and obtain that for $2\le j\le \frac{N}{2}$ and $\frac{N}{2}+1<j\le N$, $\mathrm{Re}(c_1(\mu^H_{j,\pm}(G_{la})))$ is given by (A.23) and (A.24) respectively with their corresponding $\xi_R^{(j^*)}$, $\xi_{Im}^{(j^*)}$, $\eta_R^{(j^*)}$, $\eta_{Im}^{(j^*)}$, $\tau_R^{(j^*)}$, $\tau_{Im}^{(j^*)}$, $\chi_R^{(j^*)}$, $\chi_{Im}^{(j^*)}$, $\widetilde{\xi}^{(j^*)}$, $\widetilde{\eta}^{(j^*)}$, $\widetilde{\tau}$ and $\widetilde{\chi}$. However, especially for $j=\frac{N}{2}+1$, $\mathrm{Re}(c_1(\mu^H_{j,\pm}(G_{la})))$ is given as

$$
\begin{aligned}
&\mathrm{Re}\big(c_1(\mu^H_{j,\pm}(G_{la}))\big)\\
&=\mathrm{Re}\big(\langle \boldsymbol{q}^*, Q_{\boldsymbol{w}_{11}\boldsymbol{q}}\rangle\big)+\frac{1}{2}\mathrm{Re}\big(\langle \boldsymbol{q}^*, Q_{\boldsymbol{w}_{20}\bar{\boldsymbol{q}}}\rangle\big)+\frac{1}{2}\mathrm{Re}\big(\langle \boldsymbol{q}^*, C_{\boldsymbol{q}\boldsymbol{q}\bar{\boldsymbol{q}}}\rangle\big)\\
&=\frac{1}{2\sqrt{N}}\Big(f_{uu}\widetilde{\tau}+f_{uv}\widetilde{\chi}+g_{uv}\widetilde{\tau}\Big)+\frac{3}{8N}\Big[f_{uuu}-\frac{4d_v}{\theta}\big(\cos\frac{(j-1)\pi}{N}-1\big)f_{uuv}+g_{uuv}\Big]\\
&+\frac{1}{4\sqrt{N}}\Bigg\{\Big[f_{uu}\tau_R+f_{uv}\Big(\chi_R-\frac{2d_v}{\theta}\big(\cos\frac{(j-1)\pi}{N}-1\big)\tau_R-\frac{\omega_j}{\theta}\tau_{Im}\Big)\Big]\\
&\quad-\frac{2d_v}{\omega_j}\big(\cos\frac{(j-1)\pi}{N}-1\big)\Big[f_{uu}\tau_{Im}+f_{uv}\Big(\chi_{Im}-\frac{2d_v}{\theta}\big(\cos\frac{(j-1)\pi}{N}-1\big)\tau_{Im}+\frac{\omega_j}{\theta}\tau_R\Big)\Big]
\end{aligned}
$$

$$- \frac{\theta}{\omega_j}\left[g_{uu}\tau_{Im} + g_{uv}\Big(\chi_{Im} - \frac{2d_v}{\theta}\big(\cos\frac{(j-1)\pi}{N} - 1\big)\tau_{Im} + \frac{\omega_j}{\theta}\tau_R\Big)\right]\Bigg\}. \tag{A.25}$$

References

[1] L.J. Allen, B.M. Bolker, Y. Lou, A.L. Nevai, Asymptotic profiles of the steady states for an SIS epidemic patch model, SIAM J. Appl. Math. 67 (2007) 1283–1309.

[2] M. Asllani, J.D. Challenger, F.S. Pavone, L. Sacconi, D. Fanelli, The theory of pattern formation on directed networks, Nat. Commun. 5 (2014) 1–9.

[3] A.-L. Barabási, R. Albert, Emergence of scaling in random networks, Science 286 (1999) 509–512.

[4] A. Barrat, M. Barthelemy, A. Vespignani, Dynamical Processes on Complex Networks, Cambridge Univ. Press, Cambridge, 2008.

[5] D. Brockmann, D. Helbing, The hidden geometry of complex, network-driven contagion phenomena, Science 342 (2013) 1337–1342.

[6] L. Chang, C. Liu, G. Sun, Z. Wang, Z. Jin, Delay-induced patterns in a predator-prey model on complex networks with diffusion, New J. Phys. 21 (2019) 073035.

[7] S. Chen, J. Shi, Z. Shuai, Y. Wu, Asymptotic profiles of the steady states for an SIS epidemic patch model with asymmetric connectivity matrix, J. Math. Biol. 80 (2020) 2327–2361.

[8] V. Colizza, A. Barrat, M. Barthélemy, A. Vespignani, The role of the airline transportation network in the prediction and predictability of global epidemics, Proc. Natl. Acad. Sci. 103 (2006) 2015–2020.

[9] T. Dannemann, D. Boyer, O. Miramontes, Lévy flight movements prevent extinctions and maximize population abundances in fragile Lotka-Volterra systems, Proc. Natl. Acad. Sci. 115 (2018) 3794–3799.

[10] G. Fournié, A. Waret-Szkuta, A. Camacho, L.M. Yigezu, D.U. Pfeiffer, F. Roger, A dynamic model of transmission and elimination of peste des petits ruminants in Ethiopia, Proc. Natl. Acad. Sci. 115 (2018) 8454–8459.

[11] S. Gao, L. Chang, X. Wang, C. Liu, X. Li, Z. Wang, Cross-diffusion on multiplex networks, New J. Phys. 22 (2020) 053047.

[12] W. Gou, Z. Jin, Understanding the epidemiological patterns in spatial networks, Nonlinear Dyn. 106 (2021) 1059–1082.

[13] A. Graham, Kronecker Products and Matrix Calculus with Applications, Ellis Horwood, London, 1981.

[14] I. Hanski, O. Ovaskainen, The metapopulation capacity of a fragmented landscape, Nature 404 (2000) 755–758.

[15] B.D. Hassard, N.D. Kazarinoff, Y.-H. Wan, Theory and Applications of Hopf Bifurcation, Cambridge Univ. Press, Cambridge, 1981.

[16] S. Hata, H. Nakao, A.S. Mikhailov, Dispersal-induced destabilization of metapopulations and oscillatory Turing patterns in ecological networks, Sci. Rep. 4 (2014) 3585.

[17] S.M. Hayes, K.E. Anderson, Predicting pattern formation in multilayer networks, Bull. Math. Biol. 82 (2020) 1–16.

[18] H.W. Hethcote, An immunization model for a heterogeneous population, Theor. Popul. Biol. 14 (1978) 338–349.

[19] M.D. Holland, A. Hastings, Strong effect of dispersal network structure on ecological dynamics, Nature 456 (2008) 792–794.

[20] S.-B. Hsu, On global stability of a predator-prey system, Math. Biosci. 39 (1978) 1–10.

[21] V.A. Jansen, A.L. Lloyd, Local stability analysis of spatially homogeneous solutions of multi-patch systems, J. Math. Biol. 41 (2000) 232–252.

[22] Y.A. Kuznetsov, Elements of Applied Bifurcation Theory, Springer-Verlag, New York, 1995.

[23] A. Limdi, A. Pérez-Escudero, A. Li, J. Gore, Asymmetric migration decreases stability but increases resilience in a heterogeneous metapopulation, Nat. Commun. 9 (2018) 1–8.

[24] C. Liu, L. Chang, Y. Huang, Z. Wang, Turing patterns in a predator-prey model on complex networks, Nonlinear Dyn. (2020) 1–10.

[25] H. Nakao, A.S. Mikhailov, Turing patterns in network-organized activator-inhibitor systems, Nat. Phys. 6 (2010) 544–550.

[26] H.G. Othmer, L. Scriven, Instability and dynamic pattern in cellular networks, J. Theor. Biol. 32 (1971) 507–537.

[27] H.G. Othmer, L. Scriven, Non-linear aspects of dynamic pattern in cellular networks, J. Theor. Biol. 43 (1974) 83–112.

[28] J. Petit, M. Asllani, D. Fanelli, B. Lauwens, T. Carletti, Pattern formation in a two-component reaction-diffusion system with delayed processes on a network, Physica A 462 (2016) 230–249.

[29] J. Petit, T. Carletti, M. Asllani, D. Fanelli, Delay-induced Turing-like waves for one-species reaction-diffusion model on a network, Europhys. Lett. 111 (2015) 58002.
[30] J. Petit, B. Lauwens, D. Fanelli, T. Carletti, Theory of Turing patterns on time varying networks, Phys. Rev. Lett. 119 (2017) 148301.
[31] E. Plahte, Pattern formation in discrete cell lattices, J. Math. Biol. 43 (2001) 411–445.
[32] S. Ruan, W. Wang, S.A. Levin, The effect of global travel on the spread of SARS, Math. Biosci. Eng. 3 (2006) 205.
[33] H.-B. Shi, S. Ruan, Spatial, temporal and spatiotemporal patterns of diffusive predator-prey models with mutual interference, IMA J. Appl. Math. 80 (2015) 1534–1568.
[34] Y. Shi, Z. Liu, C. Tian, Hopf bifurcation in an activator-inhibitor system with network, Appl. Math. Lett. 98 (2019) 22–28.
[35] Y. Song, T. Zhang, Y. Peng, Turing-Hopf bifurcation in the reaction-diffusion equations and its applications, Commun. Nonlinear Sci. 33 (2016) 229–258.
[36] C. Tian, Z. Liu, S. Ruan, Asymptotic and transient dynamics of SEIR epidemic models on weighted networks, Eur. J. Appl. Math. (2022) 1–24.
[37] C. Tian, S. Ruan, Pattern formation and synchronism in an allelopathic plankton model with delay in a network, SIAM J. Appl. Dyn. Syst. 18 (2019) 531–557.
[38] L. Wang, X. Li, Spatial epidemiology of networked metapopulation: An overview, Chin. Sci. Bull. 59 (2014) 3511–3522.
[39] F. Yi, J. Wei, J. Shi, Bifurcation and spatiotemporal patterns in a homogeneous diffusive predator-prey system, J. Differ. Equ. 246 (2009) 1944–1977.